InSGeP

Investigations of Slags from Next Generation Steel Making Processes

Deliverable 2.4

Modelling and simulation results

The research leading to these results has received funding from the European Union's Research Fund for Coal and Steel research programme under grant agreement number: 101112665

Project information

Project title	Investigations of Slags from Next Generation Steel Making Processes		
Project acronym	InSGeP		
Grant Agreement No.	101112665		
Project start date	01-07-2023	**Project end date**	30-06-2027

Document information

Deliverable title	Modelling and simulation results
Deliverable number	2.4
Related work package	WP2
WP leader	SSSA
Related task	2.4
Task leader	SSSA
Number of pages	49
Author(s)	Ismael Matino (SSSA), Valentina Colla (SSSA), Teresa Annunziata Branca (SSSA), Jean-Christoph Pierret (CRM), Thibaut Marcon (CRM) Marta Guzzon (Tenova), Raquel Arias Perez (Sidenor), Mattia De Colle (AMMR)
Due date	30th June 2025 (new date 31st August 2025)
Submission date	29th August 2025
Dissemination level	Public – fully open

Abstract

Deliverable 2.4 focuses on the simulation investigations carried out within InSGeP project to provide a comprehensive overview of how alternative iron bearing materials and new processes influence slag production.

For this purpose, two EAF models were employed: one stationary and one dynamic. The simulated scenarios were defined in line with requirements of industrial partners and technology providers and cover both modifications of established industrial practices through the use of HBI or DRI for producing different steel grades, and more exploratory scenarios involving also highly unconventional conditions.

Since EAF slag production and features are closely linked to both process parameters and product requirements, the simulations also monitored process and product behavior in case of DRI/HBI use.

Across the different scenarios, changes in EAF slag properties were observed and possible process adaptations to meet both product and slag specifications were considered.

In addition, an ESF flowsheet model for hot metal production was developed to investigate ESF slags behavior and its changes in case of different feedstocks. The model is under test phase and then will be used for the mentioned scenarios simulations.

List of tables

List of figures

List of abbreviations and acronyms

AC	alternating current
BF	blast furnace
DC	direct current
DR	direct reduction
DRI	direct reduced iron
EAF	electric arc furnace
ESF	electric smelting furnace
HBI	hot briquetted iron
HM	hot metal
HPSR	hydrogen plasma smelting reduction
IB	basicity index
MAPE	mean absolute percentage error
NG	natural gas
PVC	percentage variation coefficient
R&D	research and development
RFCS	Research Fund for Coal and Steel
SAF	submerged arc furnace
tls	ton of liquid steel
TRL	technology readiness level

Table of contents

1 Introduction

Next generation iron and steelmaking process aims at decreasing CO_2 by using direct reduced iron (DRI) with varying reduction degrees, hot briquetted iron (HBI), hydrogen plasma smelting reduction (HPSR) or by operating electrical smelters for low-grade ores. It will result in increase of electric arc furnace (EAF) slag and other slags with different properties. This requires understanding the possibility to valorize future slags in the present value chain and define innovative applications to assure smooth transition process without disruption to the steel industry as well as other sectors (such as road construction or cement) that currently rely on slag as raw material for their processes. To understand and move forward the transition of the steel industry, the InSGeP project is investigating slags resulting from next generation steelmaking in Europe. The project relies on the limited amount of current produced slags from next generation steel production in Europe and abroad as well as on laboratory, pilot scale and industrial scale tests that will be performed based on the needs of the involved partners.

Since, the extent of slag changes is expected to be strictly related to both feedstocks features, melting and processing unit, operating condition and produced steel grade, Deliverable 2.4 aimed at providing a more complete overview and understanding of these changes.

Deliverable 2.4 describes the modelling and simulation activities carried out to provide a more comprehensive overview of EAF slags formation, considering different feedstocks to produce different steel grades and for different EAF units. It also presents a Smelter / Electric Smelting furnace (ESF) flowsheet model for estimating slag produced during hot metal production in an ESF in case of different feedstocks.

The Deliverable includes four main sections.

- An overview of original and available EAF process models.
- Literature analyses and collected data that was used in modelling and simulations.
- EAF models adaptations that were made to make the models suitable for InSGeP needs related to simulations and ESF developed model is described.
- Simulations and results of the models.

2 Brief overview of initially available models

This section describes the original versions of the two models that have been adapted and were used in InSGeP project. The two models are a stationary flowsheet model of EAF route and a dynamic EAF metallurgical model.

2.1 Stationary flowsheet model of scrap-based EAF route

A stationary flowsheet model of scrap-based EAF route was developed by SSSA during the RFCS project EIRES[1,2] in Aspen Plus V8.4 environment. It aimed at making environmental and energetic impact evaluations in case of conventional and not-conventional production scenarios[3,4]. During the years the model was updated, improved and adapted in other European projects (i.e. iSlag[5], GreenHeatEAF[6]) for making simulations aimed at further investigations (e.g. for slag characterization[7,8], analyzing the effects of alternative carbon-bearing material in the EAF[9], checking the effects of the use of hydrogen in EAF burners[10]). Its current version exploits Aspen Plus V11.

The model considers in a modular way the main steps of electric steelmaking with discontinuous (batch) EAF until the receipt of steel in tundish and beginning of continuous casting. It allows for evaluation on a heat basis of the effects of operating conditions, charges and configuration changes. In particular, it allows estimation and monitoring the evolutions of the main process variables during different production phases: temperatures, amount and composition of steel and slags, energetic contributions, CO_2 emissions and efficiencies.

The different process steps and involved phenomena are simulated as the sum of effects in terms of materials and energetic flows and related transfers, chemical reactions, thermodynamic equilibria, phase transitions, etc. Therefore, several unit blocks are combined with each other with calculator and customized “design-specs” blocks. Since its first version, the model has been designed to be adaptable and transferable: only readily available plant data is needed for tuning, validation, and use of the models.

---

[1] GA: RFSR-CT-2013-00030, Environmental impact evaluation and effective management of resources in the EAF steelmaking - EIRES

[2] Matino, I., Alcamisi, E., Colla, V., Baragiola, S., & Moni, P. (2016). Process modelling and simulation of electric arc furnace steelmaking to allow prognostic evaluations of process environmental and energy impacts. Matériaux & Techniques, 104(1), 104.

[3] Matino, I., Colla, V., & Baragiola, S. (2017). Quantification of energy and environmental impacts in uncommon electric steelmaking scenarios to improve process sustainability. Applied Energy, 207, 543-552.

[4] Matino, I., Colla, V., & Baragiola, S. (2018). Internal slags reuse in an electric steelmaking route and process sustainability: Simulation of different scenarios through the EIRES monitoring tool. Waste and Biomass Valorization, 9(12), 2481-2491.

[5] GA: 899164, Optimising slag reuse and recycling in electric steelmaking at optimum metallurgical performance through on-line characterization devices and intelligent decision support systems, iSlag

[6] GA: 101092328, Gradual integration of renewable non-fossil energy sources and modular heating technologies in EAF for progressive CO2 decrease, GreenHeatEAF.

[7] Petrucciani, A., Zaccara, A., Matino, I., Colla, V., & Ferrer, M. (2022). Flowsheet model and simulation of produced slag in electric steelmaking to improve resource management and circular production. Chemical Engineering Transactions, 96, 121-126.

[8] Matino, I., Petrucciani, A., Zaccara, A., Colla, V., Prieto, M. F., & Pérez, R. A. (2025). Characterization of EAF and LF Slags Through an Upgraded Stationary Flowsheet Model of the Electric Steelmaking Route. Metals, 15(3), 279.

[9] Matino, I., Colla, V., Toscanelli, O., Soto, A., & Zubero, A. (2024). Esplorare l’uso di fonti alternative e non fossili di carbonio nelle acciaierie elettriche attraverso un modello flowsheet dedicato. La Metallurgia Italiana, 24.

[10] Colla, V., Matino, I., Zaccara, A., & Toscanelli, O. (2025). Simulation of hydrogen usage in electric arc furnace for its decarbonization. In AISTech-Iron and Steel Technology Conference Proceedings (pp. 2226-2233). Association for Iron and Steel Technology.

The model's modularity allows for easy integration/replacement of specific process phases/stations. This has allowed the model to be customized and used to simulate production scenarios for different steel families (groups of similar steel grades) and for different electric steelworks.

The model uses the "SOLIDS" method and related thermodynamic models for the thermodynamic calculations of most of the included units. However, some units, especially those related to the use of gas (e.g. burners), use different methods.

A list of numerous components is included in the model, and it is constantly evolving according to the needs. It includes both elements and compounds generally considered in every type of steel production with an electric cycle and in related simulations (e.g., Fe, C, CaO, FeO), as well as others more specific to certain production processes or for specific analyses (e.g., B, biomass, an alternative carbon bearing material modeled as a "non-conventional compound - NC"). This list, in fact, is the result of continuous model updates to allow for specific analyses, considering aspects requested by specific users, using the model with particular data (e.g., in the case of compositions expressed differently from the standard) or for specific needs. Therefore, not all elements and compounds are used in all simulations, and some of them are used only for specific purposes.

The model includes primary and secondary metallurgy processes, but since during InSGeP only primary metallurgy part was updated and used, only this part is described below. Related flowsheet is depicted in Section 4.1 in **Figure 6**; it is referred already to the modified version used in InSGeP. As shown in Figure 2, the model can be subdivided into different areas referring to the different phases of the process.

The charging of metallic and non-metallic materials is performed through different streams that include the composition (as mass fraction), quantity, and main thermodynamic conditions (e.g., temperature) of the materials under consideration. These streams are generally included in hierarchical blocks to better group the different types of charging. Regarding scrap, several types are included in the model and characterized by average compositions. Other types can easily be added to the model.

The various charged materials are then mixed using a dedicated mixing block and sent for melting.

The energy required for the EAF process is provided by exothermic reactions, natural gas burners, and the electric arc. The burners are simulated with a dedicated unit block representing an equilibrium reactor that minimizes Gibbs free energy. Given the combustion of hydrocarbon, the "PENG-ROBINSON" method and related thermodynamic models were used in this unit.

The electricity required by the EAF is calculated in a complementary manner to the chemical energy obtained through the exothermic reactions of the process and the combustion of natural gas. Specifically, it is estimated through a dedicated "design spec" block to ensure the specified tapping temperature. Part of the supplied energy is "removed" to simplify consideration of losses and energy efficiencies; the related parameter is adjusted based on available data or empirically.

The melting of the materials fed to the EAF is simulated by combining different units allowing material melting only if liquidus temperature is reached with provided energy.

Subsequently, materials and carbon are added to the EAF; the available materials are defined in dedicated streams grouped in a hierarchical block. The model accounts for the carbon released from the electrodes via a dedicated stream. This amount can be estimated with empirical correlations or fixed with average values, depending on the available data.

All phenomena, reactions, equilibria, separations, and material distributions occurring in the EAF are simulated by combining a series of reactors, standard and customized operating units and calculator blocks. Specifically, the reactions progresses were simulated considering reaction equilibrium

constants, reaction yields, or kinetic factors based on the reaction type and on the available information. In particular, some of these parameters are empirical or are obtained from the analyses of the industrial data, while others derive from literature or directly from the software database.

At tapping, the metal is completely separated from the slag. However, it should be noted that the separation occurs in several stages using dedicated separator blocks for simplification purposes. Slag carryover can be considered when data are available, that allow for the identification of average values or empirical correlations. At tapping, the steel and slag compositions are estimated. During tapping, material additions can be made; these are managed in the same manner as described for EAF additions.

In conclusion, the main inputs and outputs of primary metallurgy part of the model are reported in **Figure 1**.

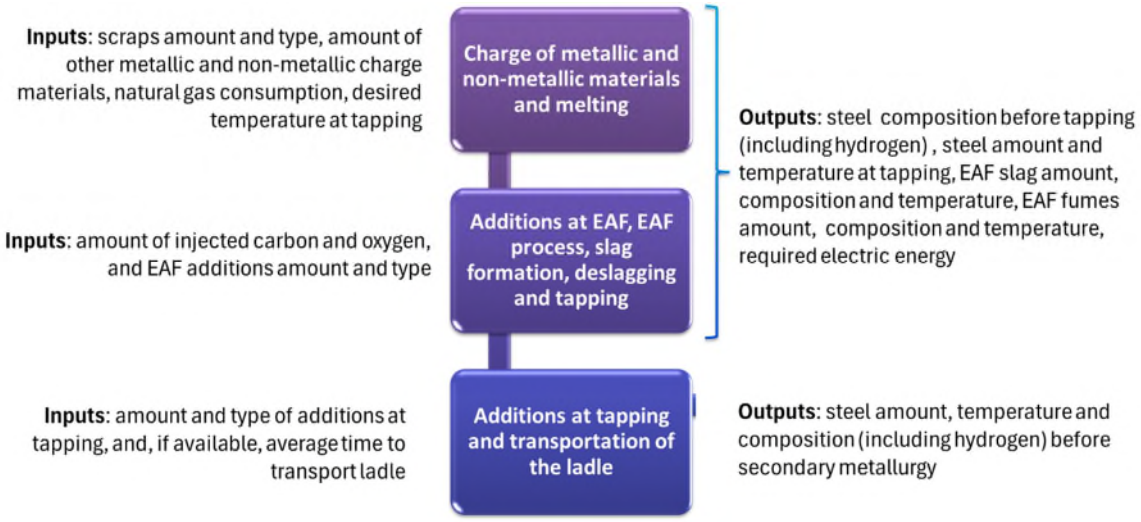

Figure 1 Inputs and outputs (on a heat basis) of primary metallurgy part of EAF route flowsheet model

The model was tuned, adapted and ad-hoc validated for different steelworks and different steel families (i.e. groups of similar steel grades) by using several amounts of heat-based data (generally data about thousands heats for each steelwork). Then, it was used for making different kinds of scenario analyses according to steelmakers' needs.

2.2 Dynamic EAF metallurgical model

The CRM EAF model is a dynamic metallurgical model that continuously solves mass and thermal balances for scrap, liquid steel, slag, gases and furnace. In addition, it calculates scrap melting evolution. The model can be applied to any furnace type (AC or DC, single or twin shell, with or without scrap preheating ...). The model is running in real time, and every time step (typically 5s) it calculates the evolution of the scrap melting in order to predict the end-point (steel carbon content and temperature) of the heat. It takes into account all process information, as well as all 'events' occurring during the heat. Particular attention has been paid taking into account all phenomena occurring during the process, such as slag foaming or metal skull formation on the bottom of the vessel.

The furnace is divided into fifteen virtual sectors, as illustrated in **Figure 2**. In each furnace sector different scrap melting rates are observed according to their relative location in the furnace. The central sector was introduced to simulate the boring phase at the beginning of the heat. In addition, each furnace sector is constituted of several scrap layers to take into account the scrap charging sequence. A

homogeneous distribution of the scrap across the furnace surface is assumed and each scrap layer follows the order inside the charged baskets. Each scrap layer is characterized by a known scrap quality (chemical composition, sterile content, density, and specific surface).

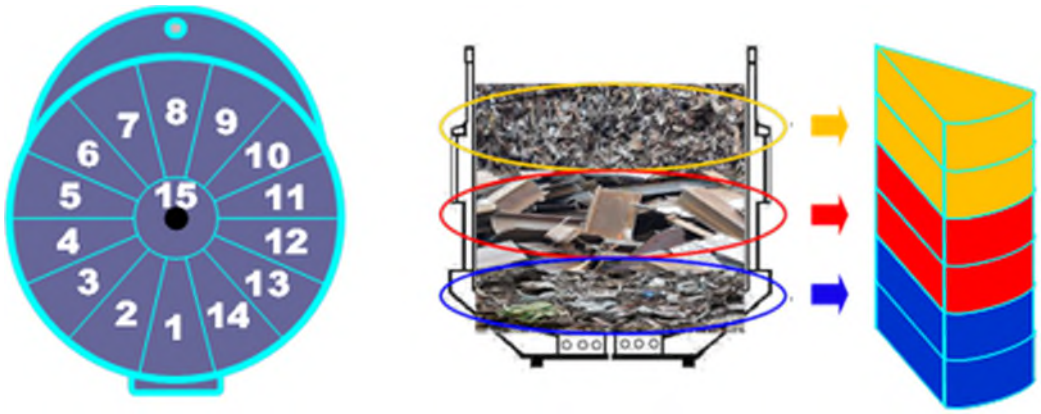

Figure 2 Furnace divided in 15 fictive sectors and sectors divided in layers

In each sector of the furnace, the scrap can be immersed in the liquid metal bath or in the slag, being subject to an intense heat exchange; the major part of the scrap charge is exposed to the gas flow ("free" scrap) in the furnace shell or in the shaft (see **Figure 3**). The parts of immersed and of free scrap vary with the progress in melting, and also depend on the liquid metal bath height and slag foaming. In case of metal skull formation, due for example to a long intermediate stop, the scrap already immersed in the bath is supposed to be 'captured' in the solidified metal on the bottom. Taking into account all energy inputs (arc, oxidation…) and mass-heat exchanges (hot gas, liquid steel bath …), the model assesses, for each layer in each furnace sector, the evolution of the scrap quantity and temperature. The model also follows the chemical and thermal evolution of the liquid bath with the scrap melting process, the oxidation reactions due to oxygen lancing and the metal-slag equilibrium.

The liquid bath is assumed to be perfectly mixed, having the same temperature and chemical composition on the whole furnace volume. The liquid metal weight varies with the scrap melting, the hot metal pouring or the reduction of the slag iron oxide. The oxidation products (CO, FeO, SiO_2 ...) are transferred to the gas or to the slag. The liquid metal bath composition evolution is assessed based on the melting progress, oxidation rates and metal-slag equilibrium.

Heat exchanges with the immersed scrap, solidified metal skull, refractory lining and slag are calculated as functions of the contact surfaces and the assumed heat transfer coefficients.

It is also calculated the chemical and thermal evolution of the slag taking into account the scrap sterile inputs, the furnace additions (lime, iron ore, anthracite …), the wear of the refractory lining and the iron oxide reduction reactions by the injected coal. The iron oxide reduction by the injected coal is determined by applying a reaction yield, the remaining amount of coal is supposed to burn in the gas. The generated carbon monoxide gas is mixed with the chamber gas and participates in the primary post-combustion reaction at the bottom of the scrap pile. In order to get a good process description the model simulates the de-slagging phenomenon, because it leads to non-negligible mass and heat losses. The wasted slag quantity is deduced based on furnace geometry, by calculating the available volumes for the foaming slag (the height of foaming slag over the slag door provides the wasted slag flow rate).

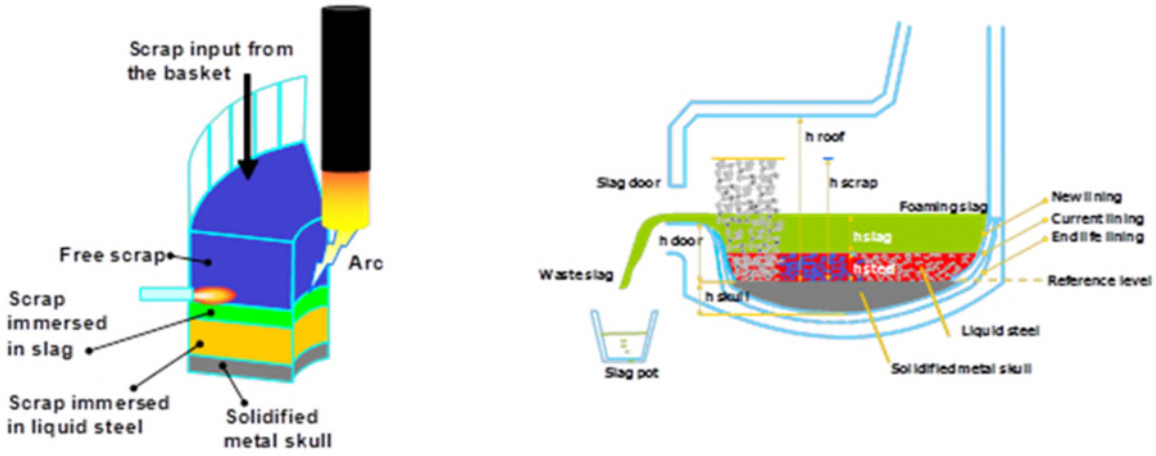

Figure 3 Possible states of scrap in a furnace sector and available volume for steel and slag

The foaming slag density varies during the melting process and depends on the carbon monoxide gas volume generated in the slag (e.g. the iron oxide reduction in the slag) and generated in the bath. The apparent foaming slag density is assessed applying an equation that takes into account the composition dependent slag density and the CO volume generated.

Other phenomena included in the calculation are:

- The solidified metal or skull formation (in case there is one) on the bottom.
- The refractory wear within the time and the thermal state of the refractory.
- The thermal losses through the refractory lining, roof, panels and offgas within the time.

The arc power distribution varies with the melting progress and depends on the volume of free scrap in the furnace. At the start of the arcing phase, the arc power is assumed to be transferred directly to the central sector until its complete melted. The arc repartition module distributes the arc power among the scrap, the liquid metal bath, the slag, the panels, the roof and the fumes. As shown in **Figure 4**, the arc power distribution varies with the melting progress and depends on the volume of free scrap in the furnace.

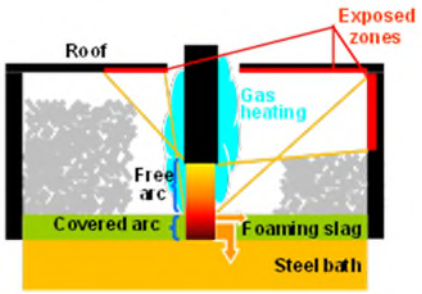

Figure 4 Arc radiation and heat transfer

The gas chemical reactions (post-combustion and air aspiration) and thermal exchanges inside the furnace are also calculated. As shown in **Figure 5**, it is simulated the primary post-combustion of the CO gas produced in the slag and the secondary post-combustion with the major part of the air ingress at the furnace door (or in the shaft inlet, in case of a scrap preheating facility). The exhaust gas collection

system module assesses the thermal exchange between the fumes and the scrap located inside the shaft (in case of scrap preheating). When available, gas composition information would allow quantifying the air ingress.

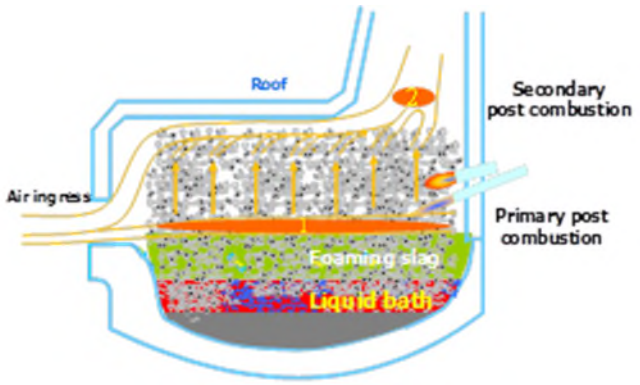

Figure 5 Gas reactions and exchanges in the vessel

The model was initially developed for 100% scrap furnace and industrially implemented. Then update to mixed hot metal / scrap charges or DRI fed plant was developed and implemented to the initial version. The model has to be compatible with the previous version for scrap melting furnaces with or without hot metal or DRI addition. The DRI module handles all the phenomena specifically associated to the DRI from charging to melting. Therefore, this module is activated only when DRI is charged into the furnace (when the flow of DRI is higher than 0). The module has been programmed taking into account previous research work done in the field of DRI melting behaviour, modelling of DRI melting and industrial experience from plant engineers and R&D. The main hypotheses adopted in this module include a reduction of the FeO in the DRI pellet to metallic Fe by the carbon contained in it at 950°C; and once molten an instantaneous separation of the metallic part (Fe, C, Si, P, etc) to the molten bath and of the oxides to the slag.

The main assumptions are summarized:

- The DRI is charged by one opening on the roof. The charged DRI is heated by radition from the arc and through contact with slag from the initial temperature to 950°C
- At 950°C most of the FeO in the DRI is reduced by the C. The heat needed for this reaction is also taken by the arc.
- After the reduction of most of the FeO the DRI pellets are heated to melting temperature and melted.
- Before melting a limited amount of the free C (around 20% of the total C) is burnt producing CO.
- Once melted the metallic part of the DRI goes to the molten bath and the oxides to the slag. Each phase will be heated to steel and slag temperature respectively.
- At a given time step, if there is not enough energy from the arc to melt all the DRI, the fraction of DRI that cannot be melted will remain solid and then melted later in the process.

The model has been calibrated for numerous industrial EAFs belonging to CRM members (ArcelorMittal plants of Belval, Dofasco, Lazaro Cardena or former Tata Steel Aldwarke EAFs) using large dataset of actual process data and measurements.

3 Literature analysis and Data Collection

Literature analysis, reported in this section, has been done to collect useful information and data. Morever, the section provides insights into the data collected from industrial partners and technology providers used for modelling and simulations.

3.1 Literature analysis

As complementary work to Deliverable 2.1 and Deliverable 2.2 of the InSGeP project and as starting point for modelling, literature analysis was carried out by SSSA on available information, correlations, data and models related to the effects that the use of alternative iron bearing materials can have on EAF process and related slags.

The data and information were investigated concerning smelting process and in particular Electric Smelting Furnace (ESF) to be used as basis for related modelling as well as for model validation.

Ehrenberg[11] provides an interesting overview on expected slag properties and chemical composition of future steelmaking route (e.g. DRI/EAF, DRI/SAF), showing their potentials and challenges to be addressed for ensuring their reuse.

Data and analysis of slag composition of EAF charged with scrap and DRI are provided by Kirschen et al.[12] together with suggestions for optimized slag operations and DRI melting process improvements.

Three plant types are studied by Gyllernram et al.[13]: an integrated plant using internal scrap, a plant using equal amounts of scrap and DRI and a plant using a smaller fraction of DRI in relation to the scrap amount. It underlines, since the amounts of gangue in DRI and foreign material in scrap both influence the performance of the EAF in a negative way, scrap upgrading should be important to keep the slag volumes at a minimum when the DRI/HBI fraction increases. The capability to cope with large slag amounts depends on the EAF design. However higher slag amounts correspond to higher iron losses, lower productivity and higher lime and energy consumption; everything affecting steelmaking economy.

A process model is proposed by Maji et al.[14] to explain the dynamic evolution of slag chemistry and foaming behavior of the slag in the early stages of EAF operations. While a static mass and energy balance model combined with a MgO saturation slag model was presented by Arzpayma[15]. Its use shows that per each 1% increase of HBI additions an increase of 34 kg in the amount of slag is obtained.

Firsbach et al.[16] analyses different technology options and processes for the defossilization of integrated plants and provides interesting information on slags. In particular, when designing a steelmaking slag, the metallurgy suggests balancing the acidic/amphoteric oxides like SiO_2 and Al_2O_3 to the desired basicity. The paper highlights how nowadays good EAF operations have around 150 kg_{slag}/t_{tap}, which

[11] Ehrenberg, A. (2023). Today's and future slags-Potentials and Challenges. ce/papers, 6(6), 241-256.
[12] Kirschen, M., Hay, T., & Echterhof, T. (2021). Process improvements for direct reduced iron melting in the electric arc furnace with emphasis on slag operation. Processes, 9(2), 402.
[13] Gyllenram, R., Arzpeyma, N., Wei, W., & Jönsson, P. G. (2022). Driving investments in ore beneficiation and scrap upgrading to meet an increased demand from the direct reduction-EAF route. Mineral Economics, 35(2), 203-220.
[14] Maji, S., & Singh, A. K. (2022). Study of slag formation and foaming in early stages of direct reduced iron (DRI)-hot metal (HM) based electric arc furnace (EAF) operation.
[15] Arzpeyma, N., Gyllenram, R., & Jönsson, P. G. (2020). Development of a mass and energy balance model and its application for HBI charged EAFs. Metals, 10(3), 311.
[16] Firsbach, F., Lückhoff, P., Schweikle, R., Pezza, A., Hansert, P., van der Velden, P., & Krause, M. Defossilization of integrated plants–benefits and challenges of different EAF designs.

lets the DR-pellet case look appealing, and the BF-pellet case inefficient - not to mention the volumes necessary inside the EAF vessel's upper shell and the amounts of slag needing transportation, processing, and selling. Concerning smelter, slag rations are smaller but with the disadvantage of significantly higher CO_2 emissions. The slag of smelters can be designed to be similar of even identical to blast furnace slag: "synthetic blast furnace slag's" basicity can be defined and targeted around 0.9 – 1.3 giving it the opportunity to be used in cements application after granulated and grinded. What is not fully understood is the role of FeO in such slag regarding the reactivity in cement. However, increasing density and a darker color can be negative aspects.

Nicholas et al.[17] shows that extra unreduced iron and gangue (impurities) could affect production yield and increase electricity consumption and slag volume in an EAF. It is highlighted that DRI melting yield in an EAF depends on the metallic iron content and level of acid gangue, silica (SiO_2) and alumina (Al_2O_3). In addition, higher iron ore content and lower gangue are preferred, more basic flux and calcium oxides (CaO) are needed to maintain the basicity of slag and to avoid excessive acid gangue (silica and alumina), which leads to more slag production and a higher amount of iron in the slag.

What has been investigated by Heo et al.[18] also presents interesting aspects. They depict that it is necessary to control amount of DRI to minimize degradation of refractory during EAF process: if a large amount of DRI must be used in the EAF process then the MgO content in the slag should be at the saturation limit at first as this accelerates the growth of the magnesiowüstite intermediate layer.

The importance of ESF in steel decarbonization is analysed by Gadd et al.[19]. A comparison between DRI-EAF and DRI-ESF route is done by Sa Ge et al.[20] through different Key Performance Indicators (KPIs), also discussing the challenges related to the control of slag chemistry related to ESF. A further comparison is done by Paymooni et al.[21]. Basic knowledge of different aspects of DRI processing is provided by Pfeiffer in its doctoral thesis[22]. Since it focuses on lower DRI grades, smelting insights are provided and slag behavior are analysed. The two step process with ESF and BOF is proposed as a more efficient solution for processing of low grade DRI compared to EAF. While operating results for three existing ESF applied to iron production using DRI are summarized in the Garlick et al. paper[23], showing the high flexibility in terms of feed quality, degree of reduction and in the ability to manage higher slag volumes.

[17] Nicholas, S., & Basirat, S. (2022). Solving Iron Ore Quality Issues for Low-Carbon Steel. Institute for Energy Economics and Financial Analysis.
[18] Heo, J., & Park, J. H. (2022). Interfacial reactions between magnesia refractory and electric arc furnace (EAF) slag with use of direct reduced iron (DRI) as raw material. Ceramics International, 48(4), 4526-4538
[19] Gadd, A., Tame, N., Liu, X., & Dukino, R. (2023). Pathways to decarbonisation episode seven: the electric smelting furnace.
[20] Ge, S., Widajat, E., Sachdeva, T., Chomyn, K., Walker, C., & Cameron, I. (2024). A Low-Carbon-Emission Flowsheet for BF-Grade Iron Ore Using Advanced Electric Smelting Furnace, in AISTech 2023 Conference Proceedings, The Iron & Steel Technology Conference and Exposition, Detroit, Mich., USA
[21] Paymooni, K., Garlick, C., Honeyands, T., & Liu, X. (2023). Simulations of DRI Integrated with EAF and ESF Processes using Beneficiated and Direct Shipment Ores, in International Symposium on Sustainable cokemaking and ironmaking, Newcaste, Australia.
[22] Pfeiffer, A. (2023). Evaluation of the Smelting Behavior of Direct Reduced Iron, Doctoral Thesis, Montanuniversität Leoben.
[23] Garlick, C., Honeyands, T., & Liu, X. (2022). Electric Smelting for Alternative Hot Metal

Further interesting papers that provide useful information for the modelling work are listed in the footnotes[24,25,26,27,28].

The CRM EAF model was already tuned to accept DRI as burden material during previous works. The ability of the model to correctly simulate actual behavior of the melting process was proved at industrial scale as could be seen in the cited references[29,30]. For the development of the "DRI" module the differences that had been included into the model are the main used references[31,32,33,34,35,36].

3.2 Data collected and used for models adaptations

SSSA received data to be used for models adaptations mainly from Sidenor and Tenova.

Sidenor provided data concerning about 400 heats produced using both scrap and HBI. They include information on the produced steel and required times, weight of charged metallic and non-metallic materials, injected O_2, natural gas and coke, 5th hole additions, additions at tapping, supplied electric energy, tapping temperature, tapped liquid metal amount, composition of liquid steel after tapping and estimate of EAF dragged slag. In addition, two HBI analyses were provided.

Further general information was also received on the characterization of steel scrap grades and its variability, the definition of tramp and valuable alloying elements requirements, EAF slags from special steels and future HBI utilization at Sidenor.

It is important to highlight that the model was previously validated for Sidenor process during two other RFCS projects (i.e. iSlag and GreenHeatEAF) with significant amount of heats data (overall more than one-thousand heats data). Therefore, data received during InSGeP were used mainly for refinement and adaptations related to the use of HBI.

[24] Kerimov, R. I., & Shakhov, S. I. (2020). Use of metallized raw materials in electric furnace steelmaking. Metallurgist, 64(1), 128-135.
[25] Dutta, S. K., Chokshi, Y. B., Dutta, S. K., & Chokshi, Y. B. (2020). Electric Furnace Processes. Basic Concepts of Iron and Steel Making, 401-496.
[26] Anderson, S. H., EDUCATED USE OF DRI/HBI IMPROVES EAF ENERGY EFFICIENCY AND YIELD AND DOWNSTREAM OPERATING RESULTS
[27] Pfeiffer, A., Wimmer, G., & Schenk, J. (2022). Investigations on the interaction behavior between direct reduced iron and various melts. Materials, 15(16), 5691.
[28] Pfeiffer, A., Ernst, D., Zheng, H., Wimmer, G., & Schenk, J. (2023). The behavior of direct reduced iron in the electric arc furnace hotspot. Metals, 13(5), 978.
[29] Lalla, N. S., González, E. F., Distefano, H., Paglialunga, M. J., Hilbert, T., & Pierret, J. C., Thermodynamics and kinetics modelling of the Electric Arc Furnace process. CRM EAF Model implementation in ArcelorMittal Acindar Plant, 24th IAS Steel Conference, Expo IAS2022, Rosario Santa Fe Argentina, 25-27 October 2022
[30] Pierret, J-C., Ojeda, C., Nyssen, P., Baumert, J-C., Thibaut, J-C., Lowry, M., Lopez, F., Lule, R., Chacon, C., Mendoza, J., & Rudiger, W. Predictive EAF model for optimisation of melting at ArcelorMittal Lazaro Cardenas, Future Steel Forum, 8-9 December 2020, online
[31] Lule, R., Lopez, F., Espinoza, J., Torres, R., & Molares, R. D. (2009). The Production of Steels Applying 100% DRI for Nitrogen Removal, the Experience of ArcelorMittal Lazaro Cardenas Flat Carbon. Proceedings of the AISTech. St. Louis, Missouri, U.S.A. (2009, Volume 1) p.467
[32] Prakash, S., Mukherjee, K., Singh, S., & Mehrotra, S. P. (2007). Simulation of energy dynamics of electric furnace steelmaking using DRI. Ironmaking & steelmaking, 34(1), 61-70.
[33] Anghelina, D., Brooks, G., & Irons, G. A. (2007). High temperature behaviour of directly reduced iron fines. Canadian metallurgical quarterly, 46(4), 373-378.
[34] Memoli, F. (2015). Behavior and Benefits of High Fe 3 C-DRI in the EAF. In Proceedings of the Association for Iron and Steel Technology Conference Proceedings, Cleveland (2015) p.1928
[35] Gupta, R. C., & Shaik, A. A. (2005). DRI apparent density and its strength. ISIJ international, 45(3), 408-409.
[36] ALEZ, O. G., AN, Y. G., Ramírez-Argaez, M. A., & Conejo, A. N. (2008). Melting behavior of simulated DRI in liquid steel. Archives of Metallurgy and Materials, 53(2).

Tenova provided mainly data on the composition of different qualities of DRI and HBI, and scrap. Data based on internal design simulations were also provided related to DRI/HBI/scrap-based EAF production; they are both related to nominal design scenarios and other specific scenarios. Insights related to Consteel® process were provided by Tenova, thanks also to several mutual discussions, that allowed adapting the model for the Consteel® related simulations.

Tenova provided useful data and indications for specific scenarios also considering highly unconventional situations.

The different data were organized and, especially in case of Sidenor heats trials data, have been clustered according to the steel families (as defined in iSlag and GreenHeatEAF projects). Afterwards, data analyses have been carried out to remove outliers and to obtain correlations and information to be used in the model adaptation and tuning stages.

A questionnaire was prepared by SSSA and shared in the consortium to acquire industrial and technology providers perspectives on plan for the steelmaking production transition, internal available models, further useful data concerning production using alternative iron bearing materials, expected scenarios to be simulated and expected models' outputs.

The data used by CRM for the calculation are based on historical industrial data from plants of the industrial partners. These initial datasets have been modified manually or using specific scripts to modify the operating pattern in order to study the influence of the parameters of interest.

4 Adapted and new models

This section describes the adaptations made to enable the use of available EAF models for the purpose of InSGeP project as well as provides the description of the developed ESF model.

4.1 Adapted stationary flowsheet model of scrap-based EAF-route

The model described in Section 2.1 required some adaptations to allow for simulations focused on DRI and HBI foreseen in InSGeP project and aimed at evaluating their effects on EAF slag, process and product. The updated flowsheet is depicted in **Figure 6**. It is a simplified flowsheet where some stream names and some customized blocks were omitted, and simplifications were inserted for a better visualization.

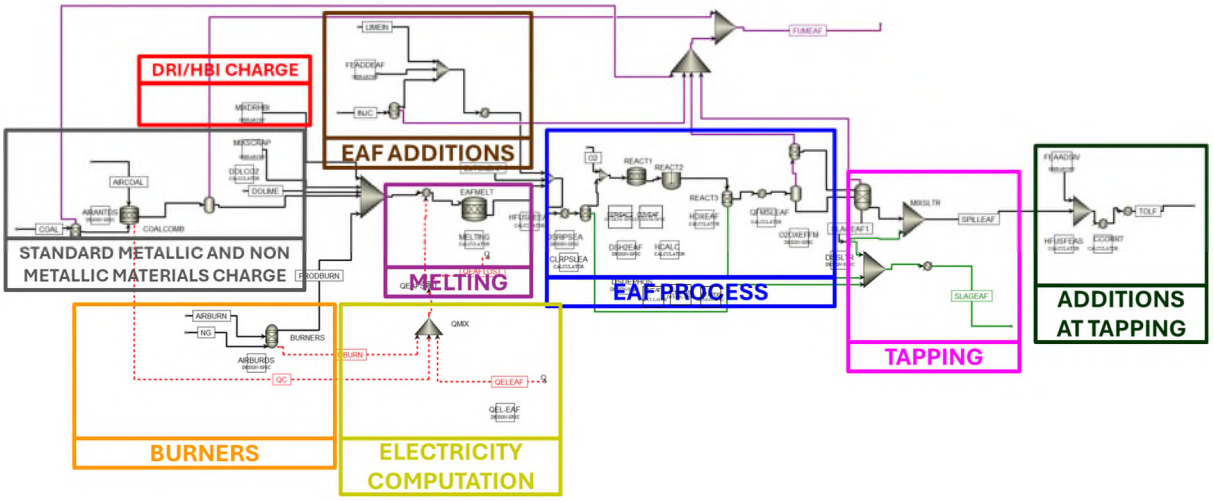

Figure 6 Flowsheet of primary metallurgy part model after adaptations for InSGeP

Among the adaptation, different streams were included in the model referring to different qualities of DRI and HBI: obtained from BF or DR grade pellets, produced using reducing gas derived from natural gas or from hydrogen rich blend, hot or cold. Collected data (see Section 3.2) were used for their characterization. The hierarchical block including all the considered alternative iron bearing materials is expanded in

Figure 7.

In order to correctly consider the effects derived from the use of DRI/HBI, the refining of the tuning of some model parameters or the inclusion of some literature/empirical relationships was done. Both literature and industrial and technology providers data were used for the scope.

Since scenario simulations were done for both batch and continuous scrap feeding processes, and considering that the original model version was conceived only for batch EAF, some further adaptations (e.g. addition of customized blocks and relationships) were needed also to better represent the continuous scrap feeding process. Finally, to allow some “design” aimed scenarios, some other modifications (e.g. addition of “design specifications” blocks) were needed to compute some process requirements by setting several slag and steel specifications.

To check the accuracy of adapted model, multiple simulations were done with data of production heats not used in the tuning phase, and original data were compared with simulation results. **Table 1** lists the

Mean Absolute Percentage Errors (MAPE) obtained from the simulated heats and refers e to the content of main compounds of EAF slag, related IB2 (CaO/SiO_2) and specific slag amounts.

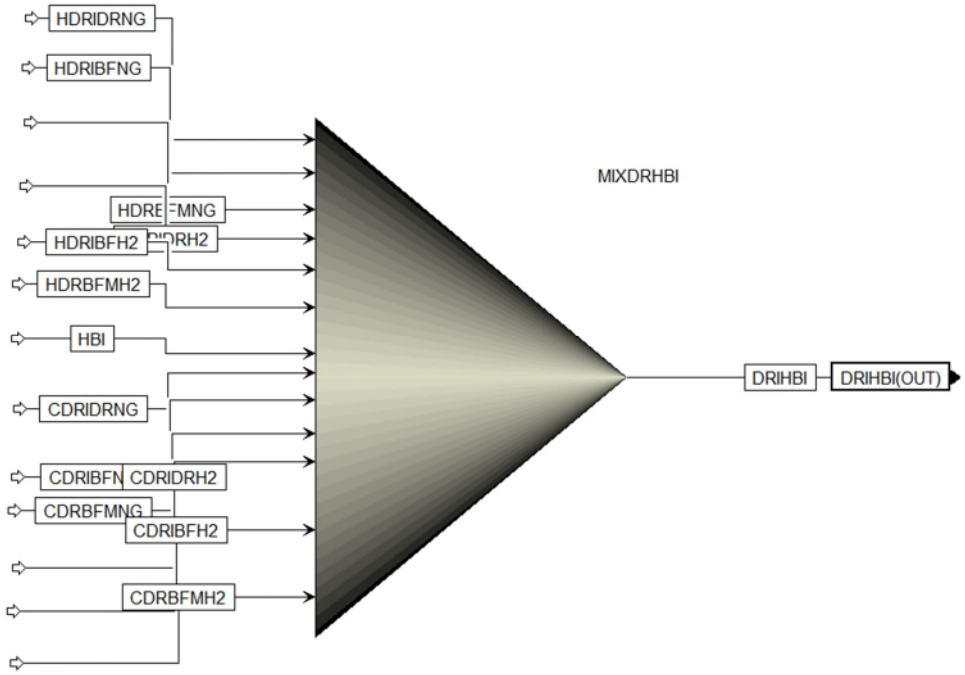

Figure 7 Hierarchical block including all the considered alternative iron bearing materials

Table 1 Adapted model test MAPE for main EAF slag variables

Variable	MAPE
FeO	11.9%
MnO	10.1%
CaO	7.2%
MgO	6.8%
Al_2O_3	15.5%
SiO_2	6.9%
IB2	3.1
Specific Slag Amount	7.9%

When excluded, Al_2O_3, MAPE is below 12% for all the listed variables. It is important to highlight that higher MAPEs generally correspond to variables showing higher Percentage Variation Coefficient (PVC). For instance, Al_2O_3, having a PCV of about 15%, shows higher MAPE than CaO or SiO_2 having PVC values of about 9% and 7%, respectively.

In addition, also for specific electricity consumption and tapped steel the accuracy of the adapted model is high: MAPEs have values of about 7.4% and 1.5%, respectively.

Continuous improvements to the model will be made during the whole duration of the project also considering the new data that will be available.

4.2 Adapted dynamic EAF metallurgical model

The CRM EAF model was already able to simulate DRI fed furnaces. This feature was developed during previous projects and validated at industrial scale on industrial partners sites (see related references in Section 3.1)). The main adaptation was to allow larger ranges of compositions of DRI and, particularly, (very) low-carbon grades (<1 % and as low as 0 %).

Additionally, some thermodynamic data has been adapted in function of C content (melting energy, auto-reduction temperature and melting temperature, kinetic parameter for carbon oxidation).

4.3 Stationary flowsheet model of ESF process

A stationary flowsheet model of ESF process was developed in Aspen Plus V14. Although theoretical[37,38,39,40,41] and literature (see Section 3.1) info and data were the bases for the model development, a significant lack of reliable and comprehensive data has been found, both from direct sources and within the existing literature. This data scarcity is related to the lower Technology Readiness Level (TRL) of the ESF technology in iron and steelmaking process with respect to the EAF one. This lack of data has made it difficult to establish a robust and validated model that can meet the required technical standards. To address the gaps, a more simplified model than the EAF one was developed. In addition, sensitivity analyses and further tests are ongoing to check the model performance and, if required, to improve it, e.g. with alternative methods of estimation.

The current model version considers the ESF in a modular way, taking into account the different main happening phenomena and reactions and allowing an easier model tuning, debugging, checking of related performances and making improvements.

The flowsheet of the current model version is depicted in **Figure 8** where the considered zones are highlighted. Similarly to the EAF case, it is a simplified flowsheet where some streams names are omitted for a better visualization.

The first zone is related to the continuous charge of materials. It includes three hierarchical blocks with feedstocks; they are related to the metallic charge with different qualities of DRI/HBI and types of scraps (see Table 3), fluxes and carbon. The amount of each charged material is defined by related design specifications blocks that allow targeting the following specifications: produced hot metal, carbon content in hot metal, slag basicity and MgO content in the slag.

The different feedstocks are charged to the top of ESF zone where there is a combination of heat exchanger, reactor and flash blocks. In this zone, where the temperature is about 1000°C, there are solid and gas phases. Some heat exchangers are used to transfer heat between the descending charged materials and the hot gases before their release. Moreover, some other heat exchangers supply part of the energy provided through the electrodes. The reactor allows beginning and partial reduction of iron oxide: both direct reduction through carbon and indirect reduction through CO are carried out. The flash unit is then used for separating the solid and gas phases.

The ESF down zone can be identified as the melting and main reactive zone; temperature of the bath depends on the specifications but it ranges of 1400-1550°C. Most of the heat provided by the electrode is delivered to the charge with a dedicated heat exchanger unit. Then, similarly to EAF model (see Section 2.1), melting is simulated through the combination of a reactor and a calculator block: the

[37] Chatterjee, A. (2014). Hot metal production by smelting reduction of iron oxide. PHI Learning Pvt. Ltd..
[38] Violi, G., (1972). Processi siderurgici, ETAS KOMPASS
[39] United States Steel Corporation. (1957). The making, shaping and treating of steel. United States Steel.
[40] Bodsworth, C. (2014), Physical Chemistry of Iron & Steel Manufacture, CBS PUBLISHERS AND DISTRIBUTORS PVT LTD
[41] Habashi, F. (1969). Principles of extractive metallurgy. Gordon and Breach.

liquidus temperature is estimated based on Carbon Equivalent Liquidus formula[42]; then if the temperature reached by the charge is greater or equal to the estimated liquidus temperature, melting of the charge is obtained. Most of the reactions are done in this zone due to the high temperatures. A dedicated reactor is used for the scope. The main reaction is the finalization of iron oxide reduction by C. Due to the high temperatures, part of MnO (if any) and less SiO_2 are reduced, passing to the liquid metal. The removal of sulfur and phosphorus are considered, but for phosphorus, the competing reduction of phosphorus oxides are also taken into account.

Each reaction considered in the top and down zones are affected by different factors, interactions and operating conditions. For this reason, a dedicated calculator block was included in the model to better consider the aspects affecting the reactions. In particular, the main effects are considered related to excess carbon rate, bath temperature, slag basicity, gangue content in DRI/HBI and DRI metallization.

The last zone considers the separation of hot metal and slag and related discharges.

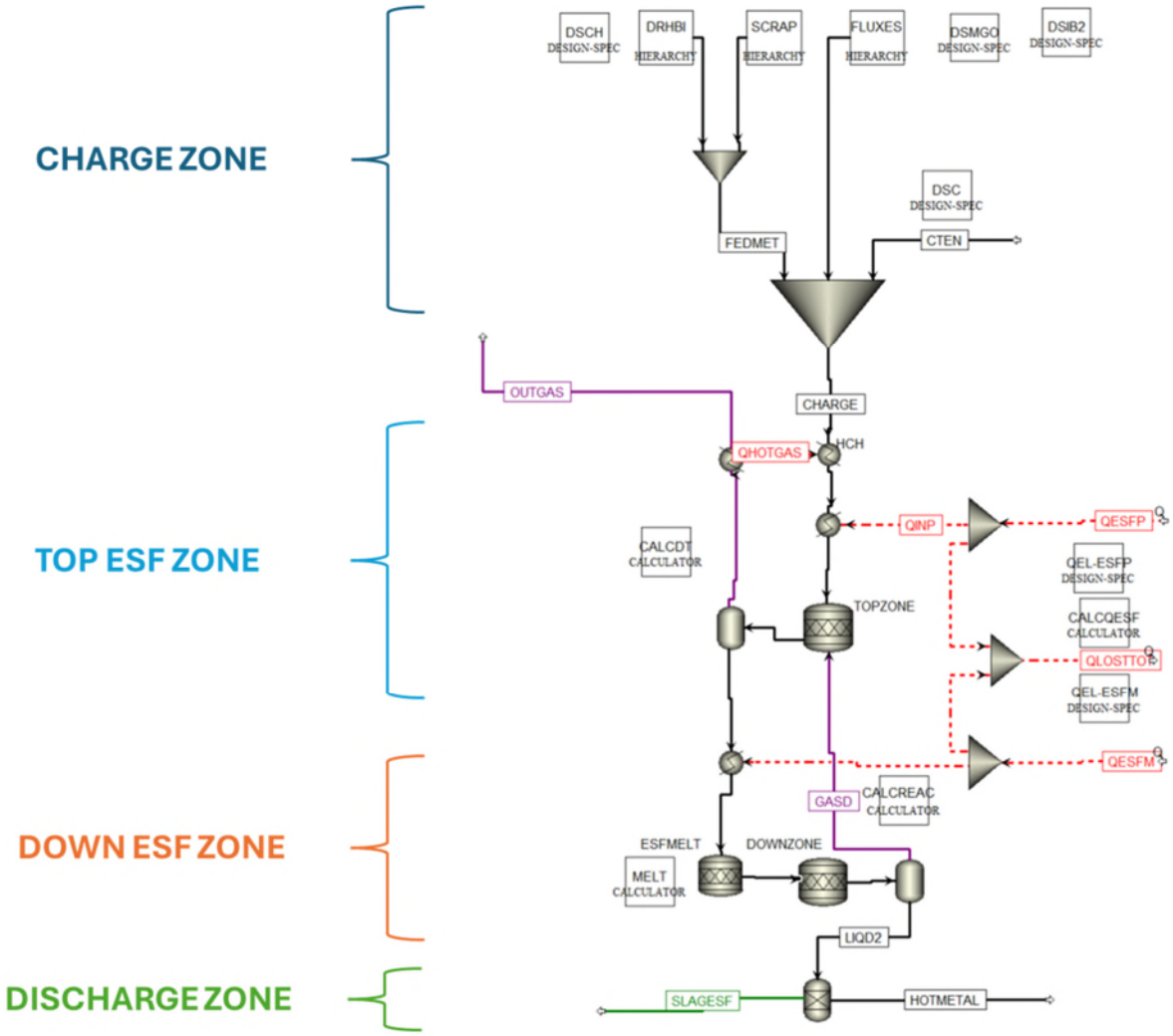

Figure 8 Flowsheet of ESF flowsheet model

[42] Heraeus Electro-Nite International N.V., (2007) Thermal Analysis of Cast Iron

Although the model is still in the test phase, an example of first comparisons of results is reported in **Table 2** considering data included in the paper by Garlick et al. (see Section 3.1).

Table 2 Example of ESF model first performances

Variable	Paper	ESF Flowsheet Model	Relative percentage error
Hot Metal			
C	3.4 wt%	4.1 wt%	20.6%
Si	0.27 wt%	0.25wt%	7.4%
Slag			
Specific Amount	190 kg/t_{HM}	189 kg/t_{HM}	0.5%
Fe_{tot}	2.8 wt%.	3.0 wt% (as 3.8 wt% of FeO)	7.1%
SiO_2	33.6 wt%	30.9 wt%	8.0%
CaO	28.4 wt%	26.0 wt%	8.5%
MgO	15.1 wt%	15.7 wt%	4.0%
Al_2O_3	19.3 wt%	22.5 wt%	16.6%
Others	n.a.	1.1 wt %	n.a.
IB2	0.85	0.84	1.2%
Specific Charged Fluxes	80 kg/t_{HM}	86 kg/t_{HM}	7.5%
Specific Offgas CO	91 Nm^3/t_{HM}	80 Nm^3/t_{HM}	12.1%

The accuracy is good, and some differences can be related to the composition and types of considered fluxes and DRI; in the considered and cited paper, fluxes compositions are not specified and DRI composition is only partially provided.

However, as previously mentioned, the model is under the test phase and if improvements are needed, they will be included before using it for scenario analyses.

5 Scenario simulations

The results of scenario simulations investigations carried out are presented in this section.

5.1 Flowsheet-based models stationary simulations

Several scenarios were simulated by SSSA to have an overview of possible consequences of the use of alternative iron bearing materials in EAF and to meet the demands of involved steelworks and technology providers. EAF slag changes were the main focus. Also process demands and main product changes in case of different EAF metallic charge, EAF type (batch or continuous), produced steel and process specifications were considered and investigated.

Some scenarios focus on consolidated industrial practices to produce different steel grades and the effects of the usage of increasing amount of HBI or DRI in them. Other scenarios are more explorative: highly unconventional situations are also considered to evaluate the effects on slags and process with different DRI qualities and produced with different reducing gases, temperatures, and by setting different specifications. In both cases, countermeasures to undesired effects are investigated

Concerning ESF, scenarios simulations will be carried out as soon as the test phase of developed model is concluded. However, the scenarios to be carried out have been defined.

5.1.1 EAF

Scenarios simulated for EAF can be grouped in the following 4 groups:

- **Scenarios A**: focused on consolidated industrial practices and aimed at checking the effect of gradual increase of HBI ratios in batch EAF charge.
- **Scenario B**: focused on consolidated industrial practices and aimed at checking the effect of gradual increase of DRI ratios in Consteel charge.
- **Scenario C**: explorative scenarios for evaluating the effect of full usage of different alternative iron bearing materials in Consteel for producing a generic low carbon steel.
- **Scenario D**: explorative scenarios for evaluating the effect of usage of a mixture of 80% wt. of scrap and 20%wt. of each alternative iron bearing materials considered in Scenario C in Consteel for producing a generic low carbon steel.

In **Scenarios A**, used HBI has the following main features: C ~ 1.3% wt., Fe (0) ~ 85.7 % wt., FeO ~8.5% wt. acidic gangue ~ 3.2% wt., basic gangue ~1.2% wt. In addition, it is important to highlight that it presents higher P content compared to the used scrap mix. The production of different steel grades belonging to different steel families has been simulated. With respect to standard industrial practice using only scrap (reference case), during this scenario, the change in HBI ratios in the charge is done while ensuring the same amount of fed iron with respect to the reference case. In addition, in order to be able to observe HBI effects, all the other process operating conditions and input materials still were held to the values that are generally exploited in the standard industrial practices where only scraps are used. Different interesting results were obtained, as exemplary reported in **Figure 9** and **Figure 10**. depicting the results for a heat belonging to Carbon Quenched and Tempered steel family. As expected, EAF specific slag amount (**Figure 9**) increases by charging more HBI in EAF because of its gangue content and incomplete metallization. These affect also the slag composition (**Figure 9**): noticeable increase of SiO_2 content was observed together with a decrease of CaO and MgO content and an increase of FeO content. Because of this composition change, an acidification of slag is observed

through the basicity index expressed as IB4=(CaO+MgO)/(SiO_2+Al_2O_3). This acidification leads to an increase of P content in tapped steel (**Figure 10**) and, although not reported in figure, to a slight increase of S content (affected also by the FeO content increase). On the other hand, C content in tapped steel was negligibly affected. Reported results well represent also the results obtained for other simulated heats for which similar behavior is observed.

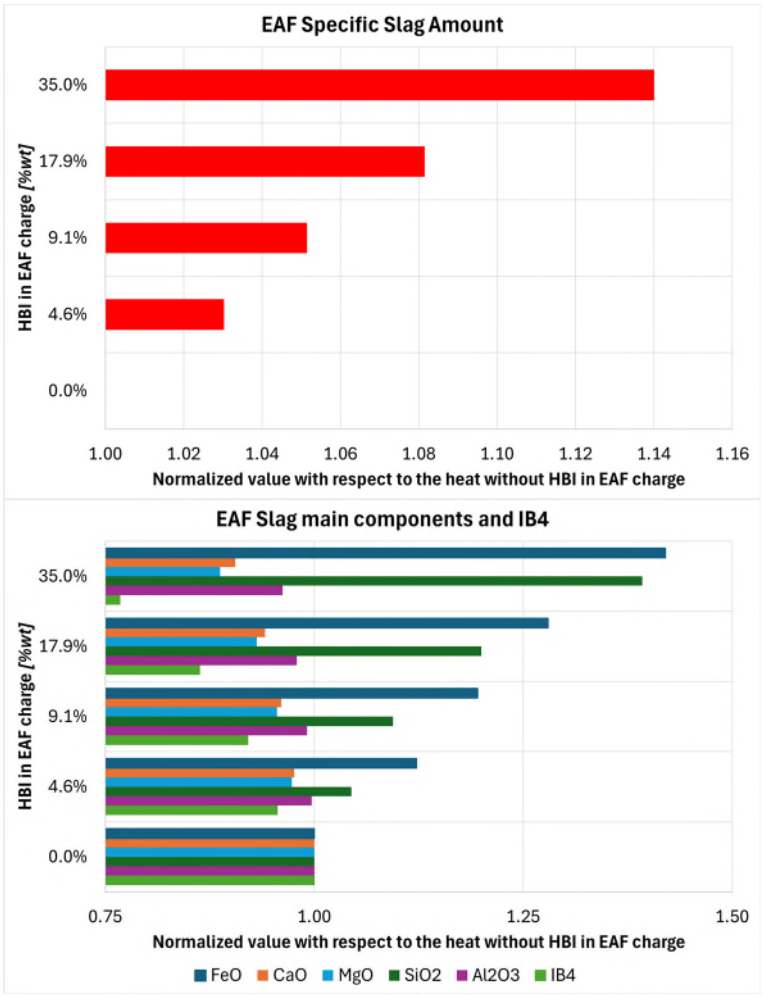

Figure 9 EAF slag results in an exemplary production heat simulated for **Scenarios A** for a steel belonging to CQ&T steel family – values are normalized for confidentiality reasons

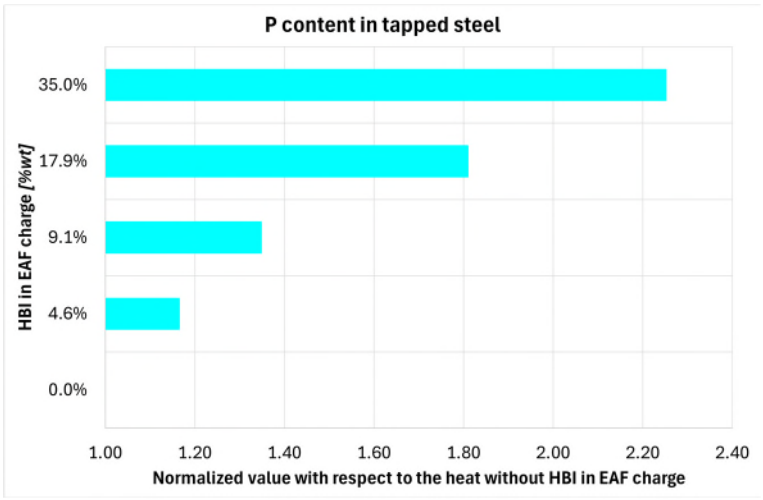

Figure 10 Effects on P content in tapped steel in an exemplary production heat simulated for **Scenarios A** for a steel belonging to CQ&T steel family – values are normalized for confidentiality reasons

Due to the observed increase of P content in tapped steel, some **Subscenarios A** were simulated, finalized at ensuring desired P content in tapped steel also with increased usage of HBI. Therefore, an increased amount of flux compounds (in particular, dolomitic lime) is charged for counteracting slag acidification with increased HBI usage. **Figure 11, Figure 12 and Figure 13** depict exemplary results of the increase of flux compounds for the same heat, whose results are reported in **Figure 9** and **Figure 10**, for scenario A, while **Figure 14, Figure 15 and Figure 16** show representative results for a further heat belonging to the Microalloyed steel family.

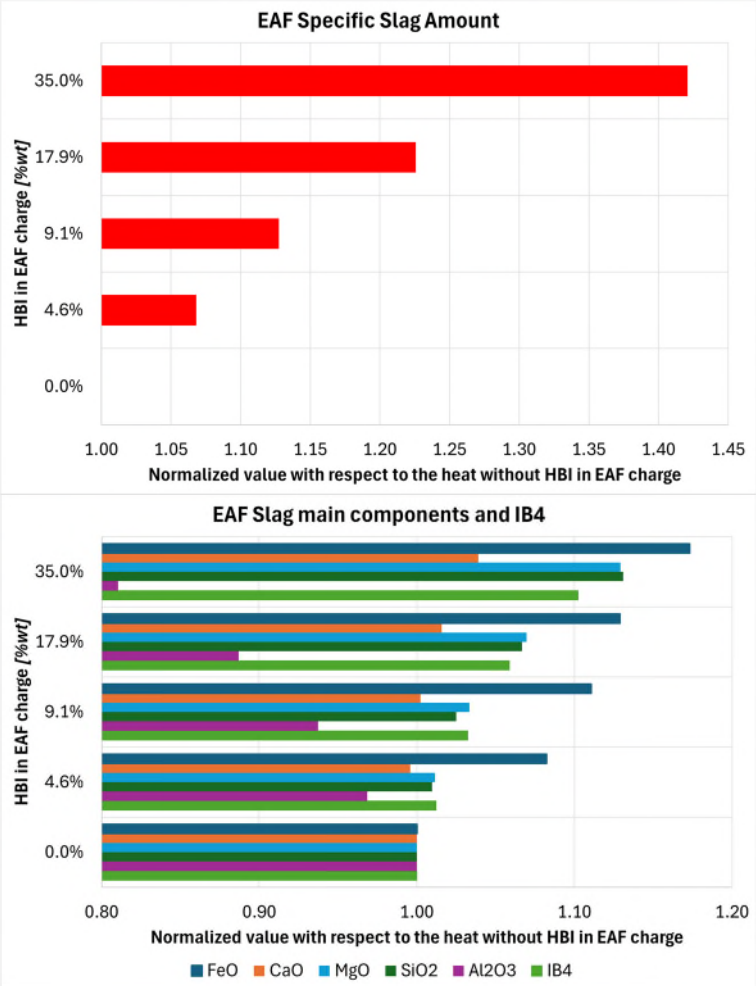

Figure 11 EAF slag results in an exemplary production heat simulated for **Subscenarios A** for a steel belonging to Carbon Quenched & Tempered steel family – values are normalized for confidentiality reasons

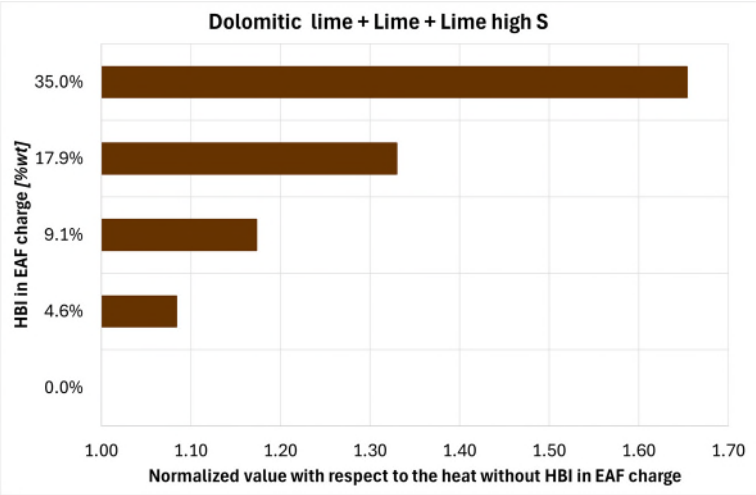

Figure 12 Effects on fluxes needs in an exemplary production heat simulated for **Subscenarios A** for a steel belonging to Carbon Quenched & Tempered steel family – values are normalized for confidentiality reasons

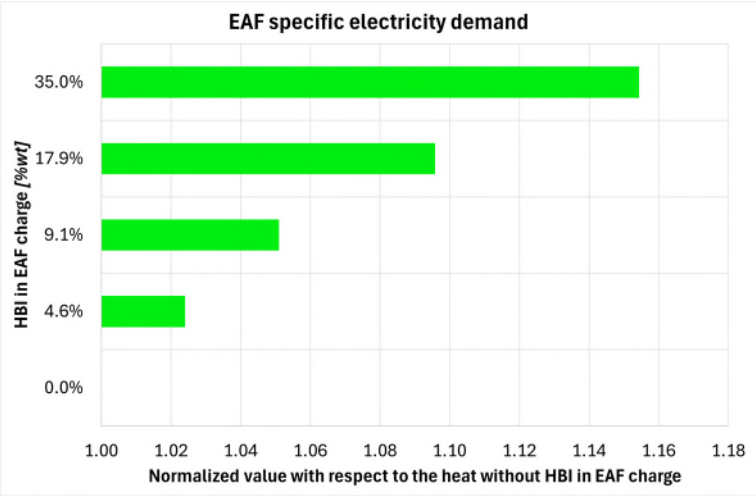

Figure 13 Effects on EAF specific electricity demand in an exemplary production heat simulated for **Subscenarios A** for a steel belonging to Carbon Quenched & Tempered steel family – values are normalized for confidentiality reasons

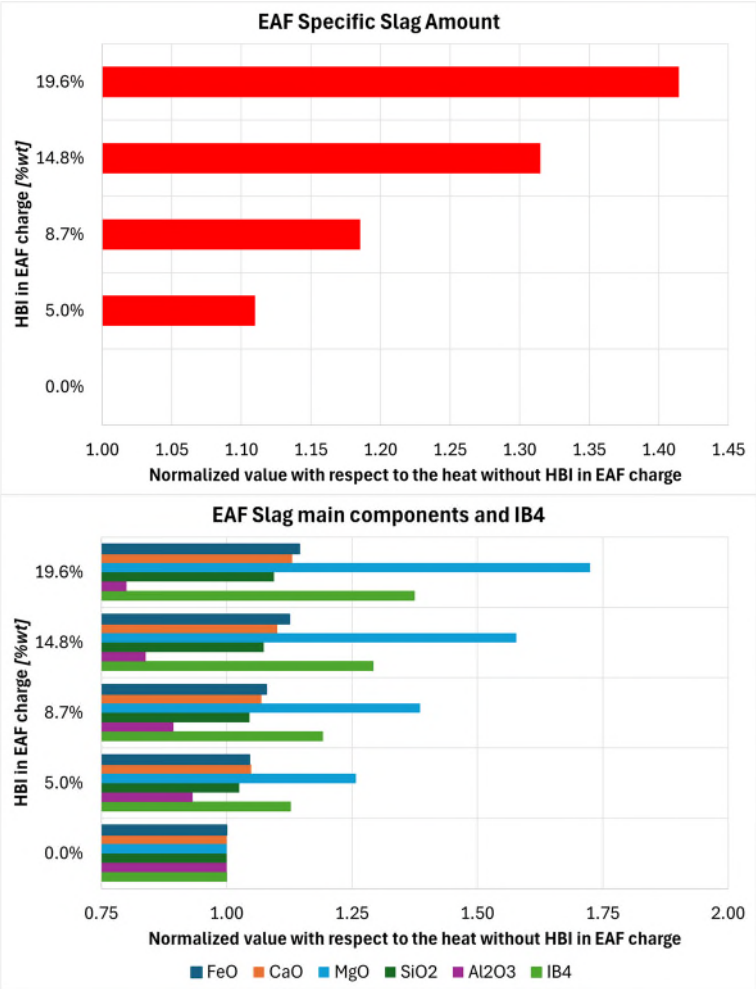

Figure 14 EAF slag results in an exemplary production heat simulated for **Subscenarios A** for a steel belonging to Microalloyed steel family – values are normalized for confidentiality reasons

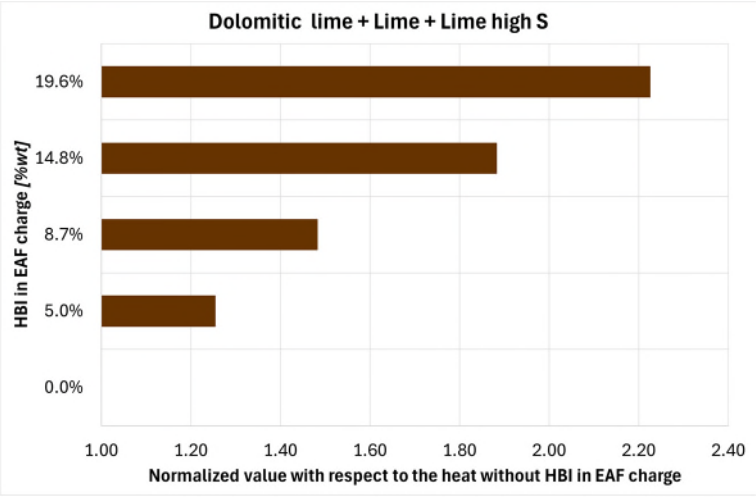

Figure 15 Effects on fluxes needs in an exemplary production heat simulated for **Subscenarios A** for a steel belonging to Microalloyed steel family – values are normalized for confidentiality reasons

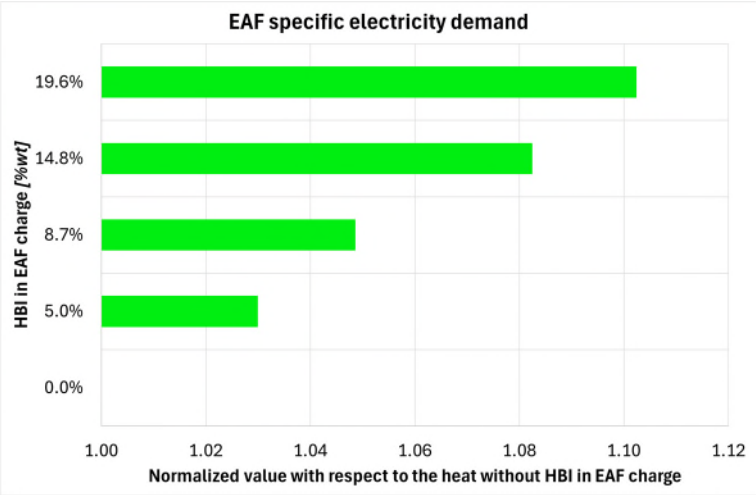

Figure 16 Effects on EAF specific electricity demand in an exemplary production heat simulated for **Subscenarios A** for a steel belonging to Microalloyed steel family – values are normalized for confidentiality reasons

In both cases, an almost linear increase of flux compounds (**Figure 12** and **Figure 13**) is needed for counteracting the acidification of the slags; however, although similar behavior for different steel families, the required additional flux compounds amount is dependent to the produced steel. As desired, an increase use of flux compounds to counteract the negative HBI effects is reflected in a EAF slag (**Figure 11** and **Figure 14**), having a more stable basicity with respect to what shown in scenarios A because the increase of acidic compounds (e.g. SiO_2) is thwarted by increasing the CaO and MgO contents. The slight IB4 increase is needed to counteract the higher charged P with increased amount of used HBI. Slag composition changes are then dependent on the produced steel. However, in any cases, EAF specific slag amount increases more than in Scenarios A, due to the increase of flux compounds. Moreover, an increase in electric energy demand was observed, as highlighted in **Figure 13** and **Figure 16**. Similar behaviors/trends were obtained also for other simulated heats and for different steel families.

Scenarios B were carried out in a similar way to **Scenarios A** but it is referred to the Consteel-based production of another steel grade and to the increase of charged DRI instead of HBI.

In particular, a mix of BF- and DR- grades DRI produced by using a high H_2 ratio in reducing gas is used. The DRI mixture has a BF-/DR- grade ratio of about 2:1 and the following main features: C ~ 0.6% wt., Fe (0) ~ 85.0 % wt., FeO ~7.0% wt. acidic gangue ~ 4.1% wt., basic gangue ~2.7% wt.. In addition, in this case, DRI holds a lower P content compared to the used scrap mix.

Similarly to the use of HBI, and as reported in **Figure 17**, EAF specific slag amount increases with higher DRI in EAF charge because of DRI gangue content and incomplete metallizzation. It can be observed a noticeable increase of the acidic compounds (i.e. SiO_2 and Al_2O_3) and of FeO in EAF slag, accompanied by a decrease of CaO content and by an acidification of slag, this time showed with IB3= $CaO/(SiO_2+Al_2O_3)$. The variations of P and S contents in tapped steel are not reported in figures because they are negligible. Moreover, a slight increase in C content is observed when increasing the DRI amount in the EAF.

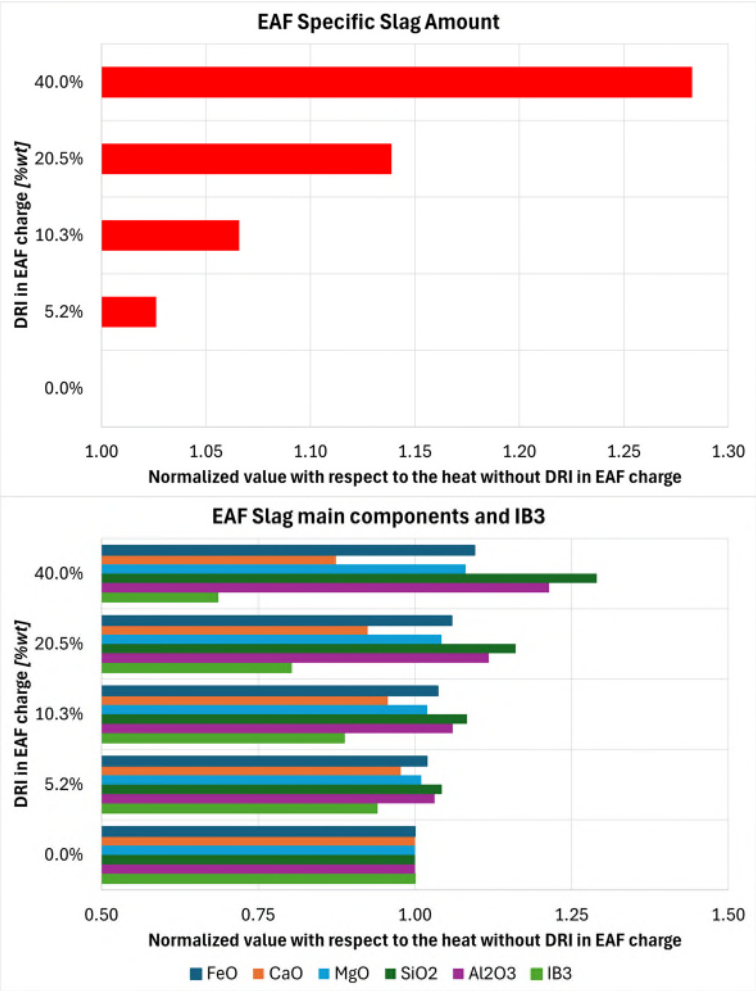

Figure 17 EAF slag results in an exemplary production heat simulated for **Scenarios B** – values are normalized for confidentiality reasons

Since in **Scenarios B** with respect **Scenarios A**, there were no significant changes in tapped steel, **Subscenarios B** were dedicated to the investigation of the flux amount required (in particular dolomitic lime) to avoid the undesired decrease of IB3 since acidification of slag affects negatively the slag properties (e.g. viscosity). As shown in **Figure 18**, a significant increase of fluxes is required to keep the IB3 constant. This significantly affects the slag composition with a high relative increase of MgO content and the produced slag amount (see **Figure 19**). Furthermore, although not reported in figures, about 4% more electric energy is required with this process conditions in case of 40% wt.% of DRI mix in the EAF charge.

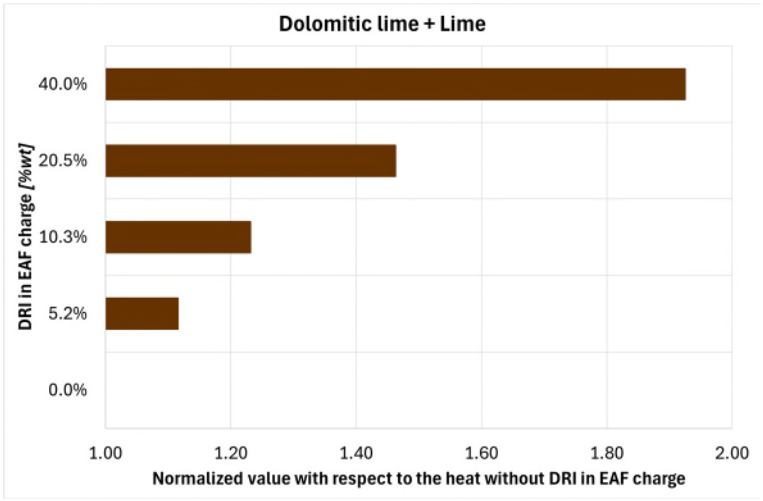

Figure 18 Effects on fluxes needs in an exemplary production heat simulated for **Subscenarios B** – values are normalized for confidentiality reasons

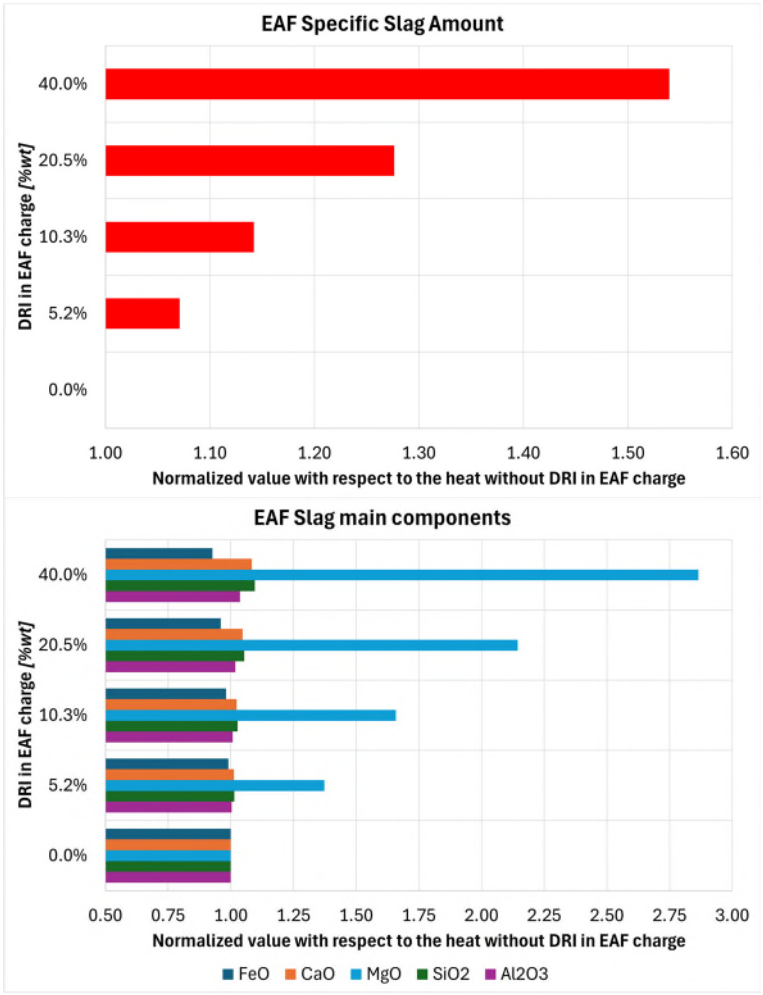

Figure 19 EAF slag results in an exemplary production heat simulated for **Subscenarios B** – values are normalized for confidentiality reasons

Scenarios C and **D** were carried under the following specifications:

- Desired amount of tapped steel = 200 tls
- C content in tapped steel = 0.04% wt
- MgO content in EAF slag = 12% wt
- IB2=CaO/SiO_2 = 2.15
- Temperature at tapping = 1650°C

The tested metallic feedstocks are listed in **Table 3** with their main features, including reducing gas and pellet used for producing them.

Table 3 Tested metallic feedstocks in **Scenarios C** and **D** and related features

Metallic charge material	Reducing Gas	Pellet	C	Fe (0)	Acidic gangue	Basic gangue	Temperature
			% wt				*°C*
Scrap A (high purity)	n.a.	n.a.	0.06	~99	n.a.	n.a.	360 (preheated in Consteel)
Scrap B	n.a.	n.a.	0.14	~96	n.a.	n.a.	360 (preheated in Consteel)
hDRI – NG – HG – C4	Natural Gas based	67.5% wt Fe DR pellet	4.00	~84	~2.7	~1.0	575
hDRI – NG – HG – C2	Natural Gas based	67.5% wt Fe DR pellet	2.00	~86	~2.7	~1.0	600
hDRI – NG – MG – C4	Natural Gas based	65% wt. BF pellet	4.00	~80	~4.6	~1.8	575
hDRI – NG – MG – C2	Natural Gas based	65% wt. BF pellet	0.70	~82	~4.7	~1.9	600
hDRI – H2 – HG	H_2+NG based	67.5% wt Fe DR pellet	0.70	~87	~2.8	~1.0	600
hDRI – H2 – MG	H_2+NG based	65% wt. BF pellet	2.00	~83	~4.7	~1.9	600
cDRI – NG – HG – C2	Natural Gas based	67.5% wt Fe DR pellet	2.00	~86	~2.7	~1.0	25
cDRI – NG -MG – C2	Natural Gas based	65% wt. BF pellet	2.00	~82	~4.7	~1.9	25
cDRI – H2 – HG	H_2+NG based	67.5% wt Fe DR pellet	0.70	~87	~2.8	~1.0	25
HBI	H_2+NG based	65% wt. BF pellet	0.70	~83	~4.7	~1.9	25

The simulations' results concern the amount of metallic charge, lime, dolomitic lime, coal charge+injected carbon and oxygen required for respecting the previously listed specifications. In addition, they gave insight on the obtained amount of EAF slag and related composition.

Concerning **Scenarios C**, the required specific metallic charge for obtaining the same tapped steel amount increases with lower quality DRI/HBI, as depicted in **Figure 20**.

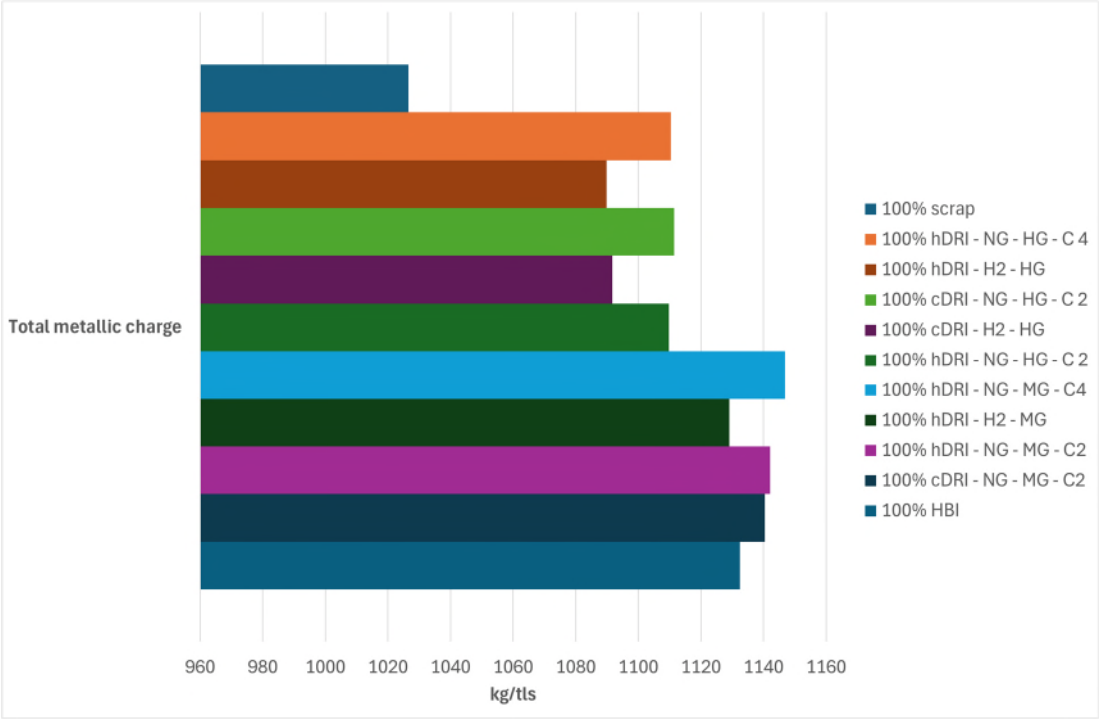

Figure 20 Variation of specific total metallic charge with different type of iron bearing materials (**Scenarios C**)

Figure 21 shows the variation of the other specific inputs with the different type of charge. Higher oxygen amount is required in different cases:

- higher C in the charge because higher decarburation is required;
- lower quality DRI/HBI because higher impurities and lower metallization have to be managed;
- cold DRI/HBI because higher chemical energy is required.

Regarding coal+injected carbon, higher amount is required in the following cases:

- lower C in the charge for allowing a higher carburization;
- cold DRI/HBI again for providing higher chemical energy;
- higher FeO in the charge because higher Fe reduction is needed.

Burned lime request increases for lower quality DRI/HBI for counteracting the higher slag acidification.

Finally higher amount of dolomitic lime is required in case of each alternative iron bearing material.

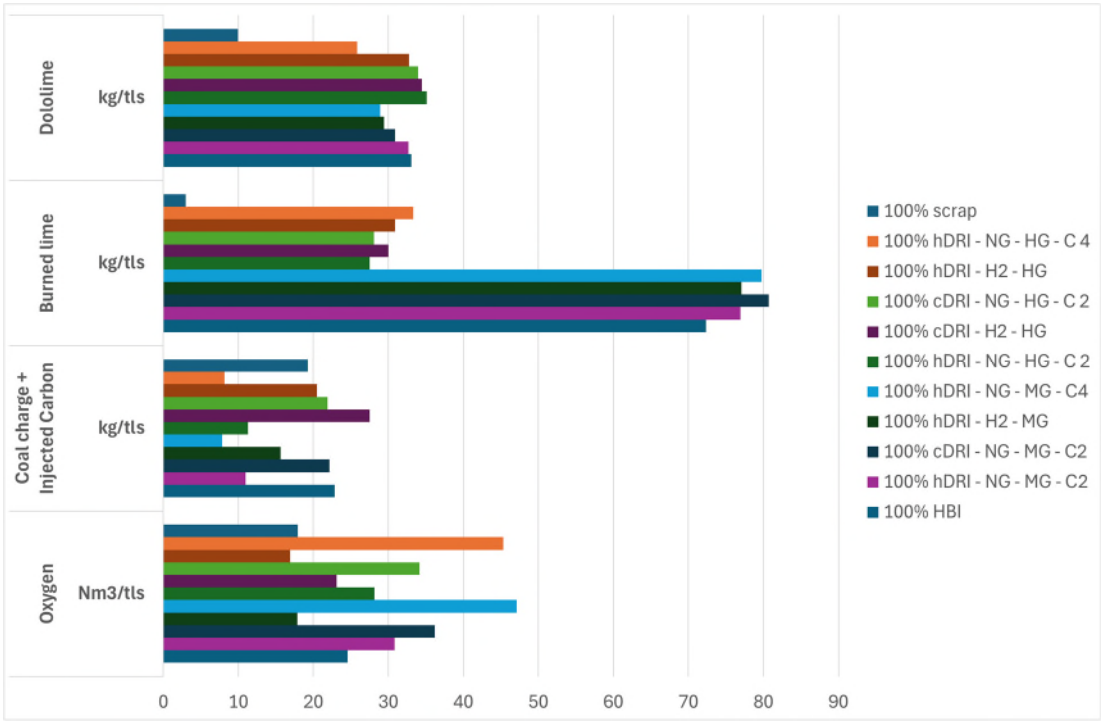

Figure 21 Variation of other specific inputs with different type of iron bearing materials (**Scenarios C**)

The effects on specific slag amount and related compositions are depicted in **Figure 22** and **Figure 23** respectively.

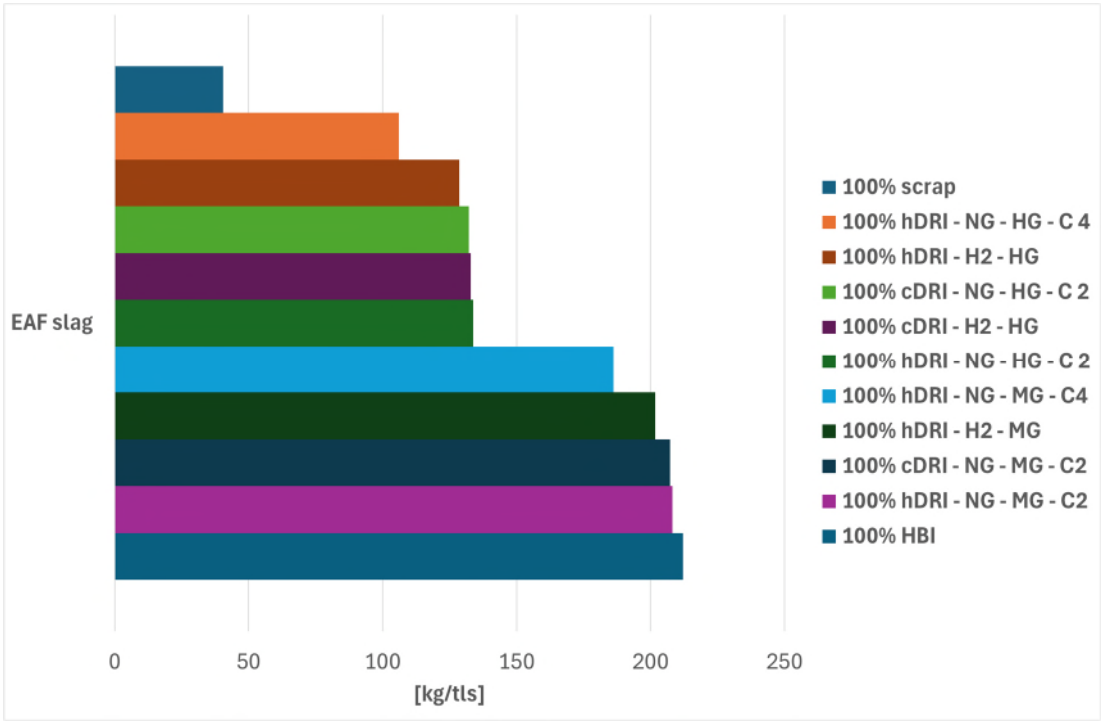

Figure 22 Variation of specific EAF slag amount with different type of iron bearing materials (**Scenarios C**)

As expected, specific EAF slag amount increases with lower quality DRI/HBI following the order reported in **Figure 22**. It is important to highlight that the high purity charged scrap results in low amount of obtained slag; synthetic slag could be necessary for operational reasons.

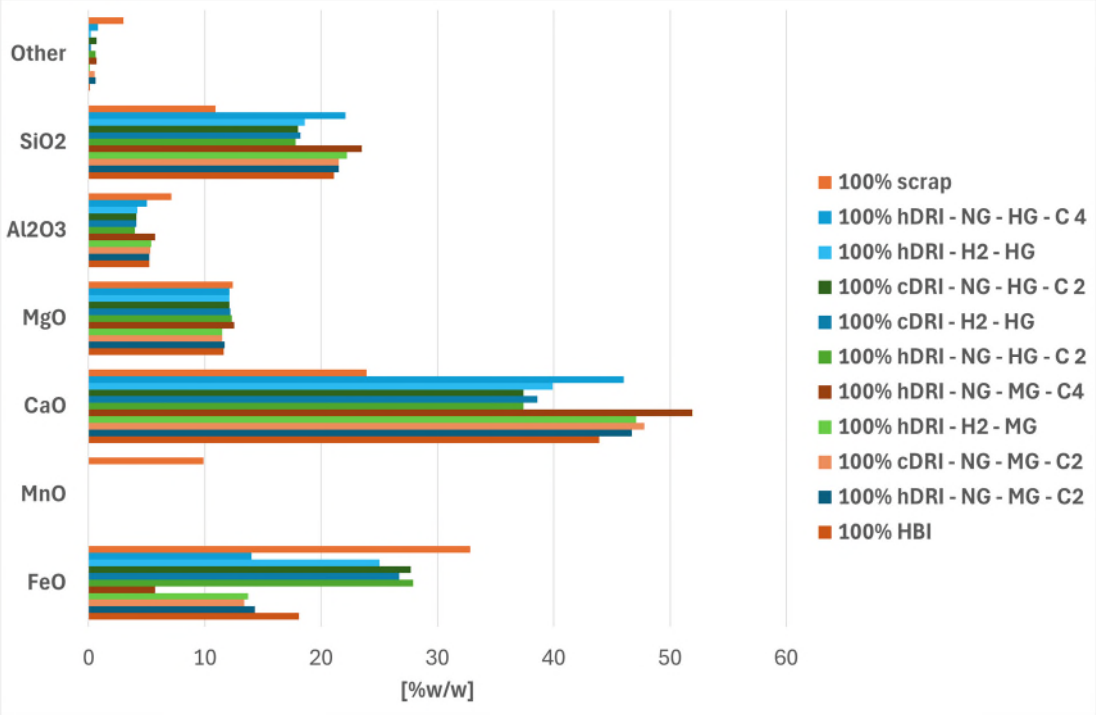

Figure 23 Variation of EAF slag composition with different type of iron bearing materials (**Scenarios C**)

Regarding slag composition the following considerations can be done:

- MnO can be found only in scrap-based EAF slag because there is no Mn in considered DRI/HBI
- SiO_2 is higher for lower quality DRI/HBI
- CaO content counteracts acidic gangue and therefore is higher for lower quality DRI/HBI
- For DRI/HBI charges, FeO is higher for lower quality iron bearing materials due to their incomplete metallization
- MgO is constant to the set value

It is important to highlight that some of the obtained slags (e.g. when a very low FeO content is obtained) with provided specifications are not suitable for correct industrial operations. To investigate the process changes required to obtain suitable slags, **Subscenarios C** were performed when obtained FeO in slag was below 25 wt-% by setting a further specification related to the content of FeO in the slag at a value of 28 wt-%.

Related results are reported in **Figure 24, Figure 25, Figure 26 and Figure 27**. Targeting the FeO content in slag (whole composition is in **Figure 27**) is translated in a higher injected oxygen (**Figure 25**) with respect to Scenarios C; it favours the FeO oxidation decreasing the metallic yield as can be observed in **Figure 24** where more specific metallic charge is needed. Moreover, for respecting the other slag specifications, more dolomitic lime is required to achieve set MgO content. This allows also decreasing charged lime for obtaining desired IB2, since more CaO is provided through the increased

MgO charged. All these process changes, while allowing for the production of an industrial operational suitable slag, lead to an increase of produced slag to be managed (**Figure 26**).

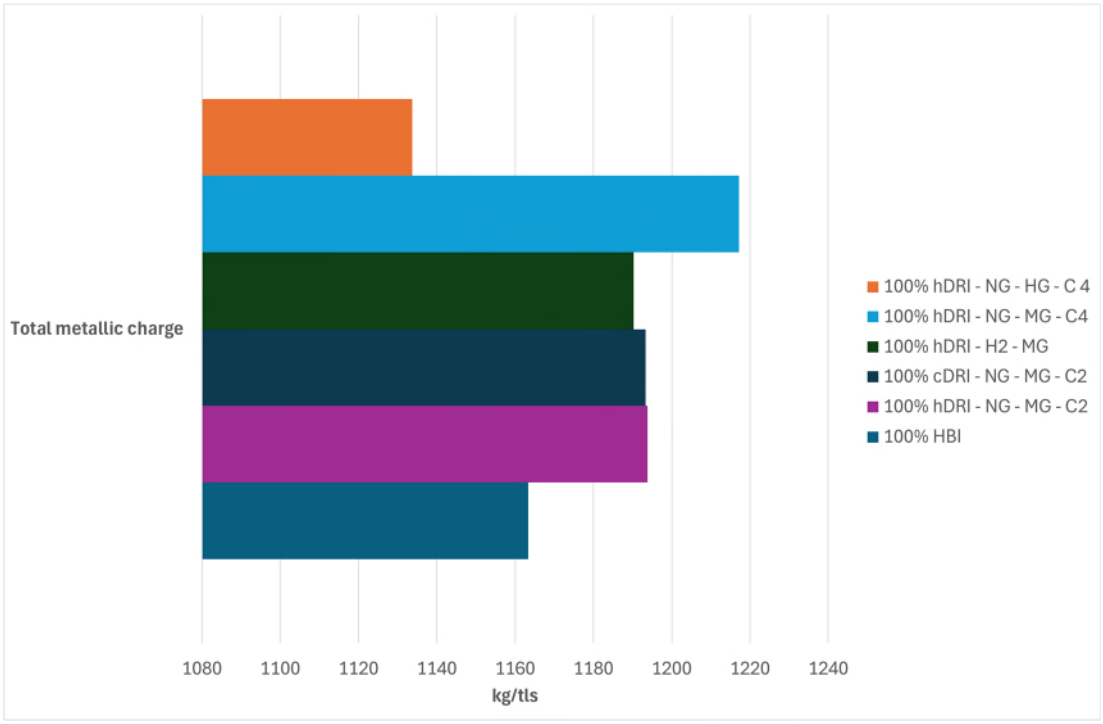

Figure 24 Variation of specific total metallic charge with different type of iron bearing materials (**Subscenarios C**)

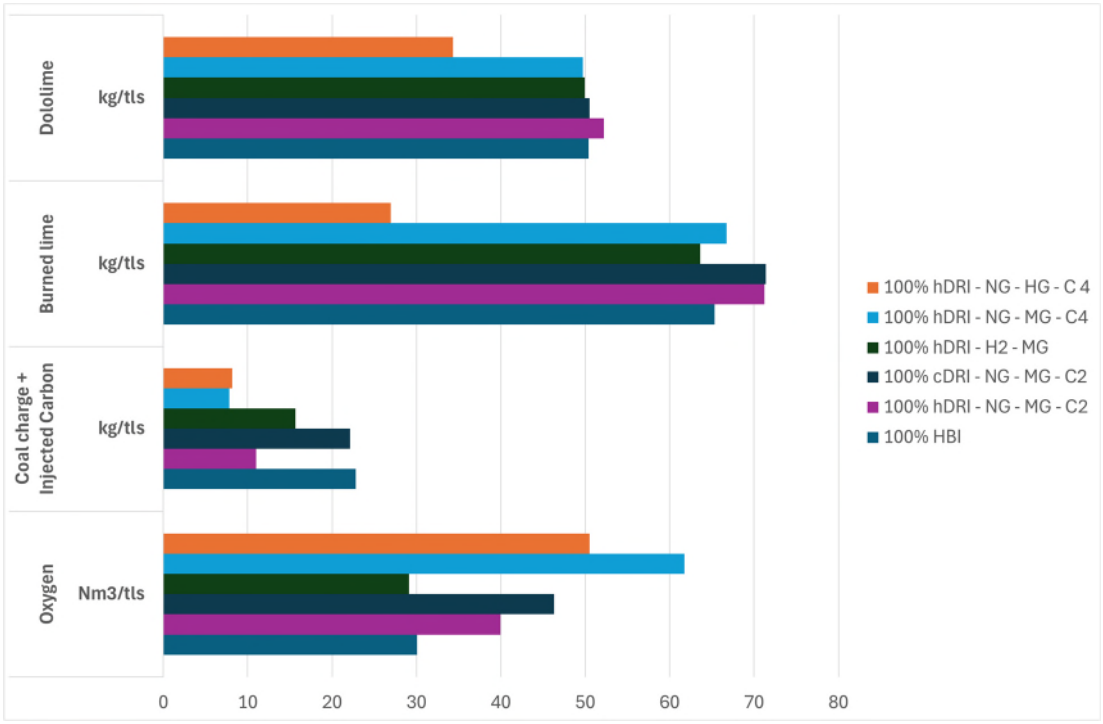

Figure 25 Variation of other specific inputs with different type of iron bearing materials (**Subscenarios C**)

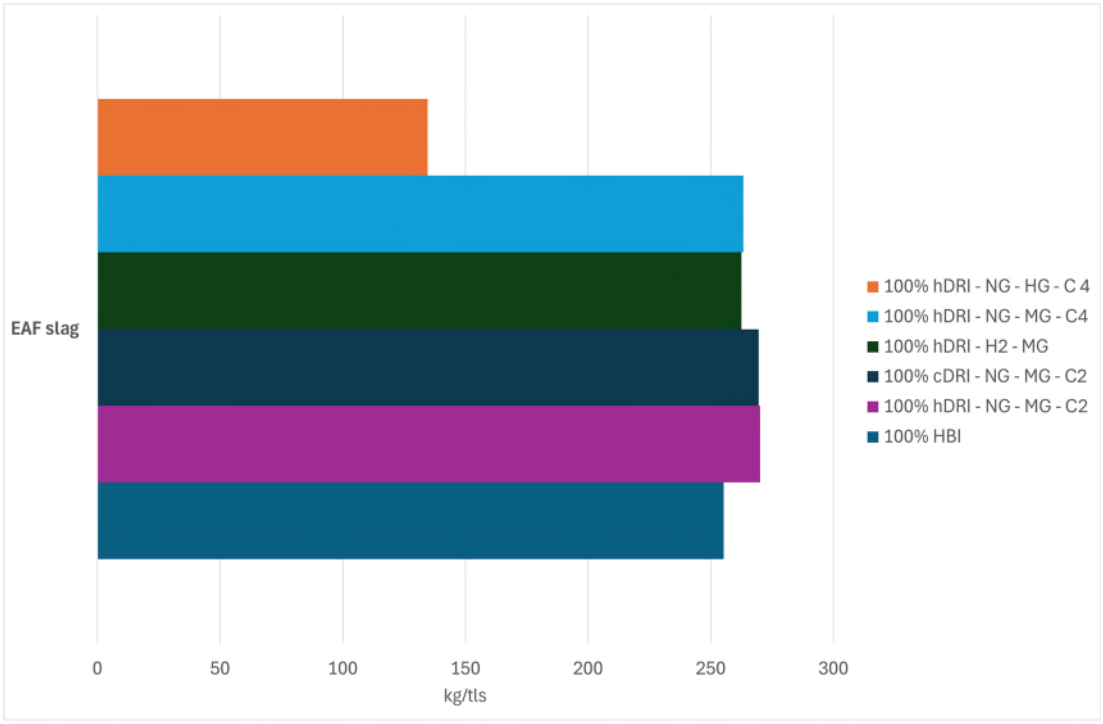

Figure 26 Variation of specific EAF slag amount with different type of iron bearing materials (**Subscenarios C**)

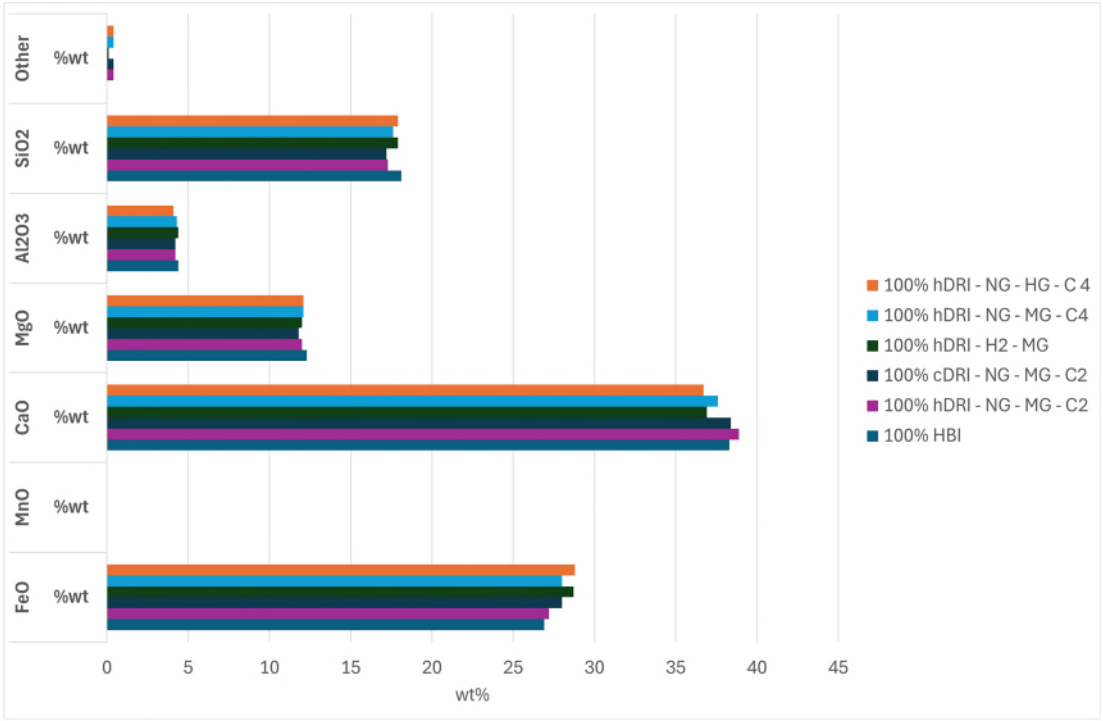

Figure 27 Variation of EAF slag composition with different type of iron bearing materials (**Subscenarios C**)

Scenarios D, where 40% wt. of scrap A (see **Table 3**) and 40%wt. of scrap B (see **Table 3**) are mixed with a limited amount of DRI/HBI, shows similar behaviors and trend of **Scenarios C** where a single type of charge is used. However, using only 20% wt. of DRI/HBI the effects are limited, as can be

observed in **Figure 28**, **Figure 29**, **Figure 30** and **Figure 31** depicting **Scenarios D** results. Main differences with respect to scrap-based production, can be observed in required burned lime and in injected oxygen. Concerning slags, amount and composition variations are limited, and all the obtained slags are operationally feasible.

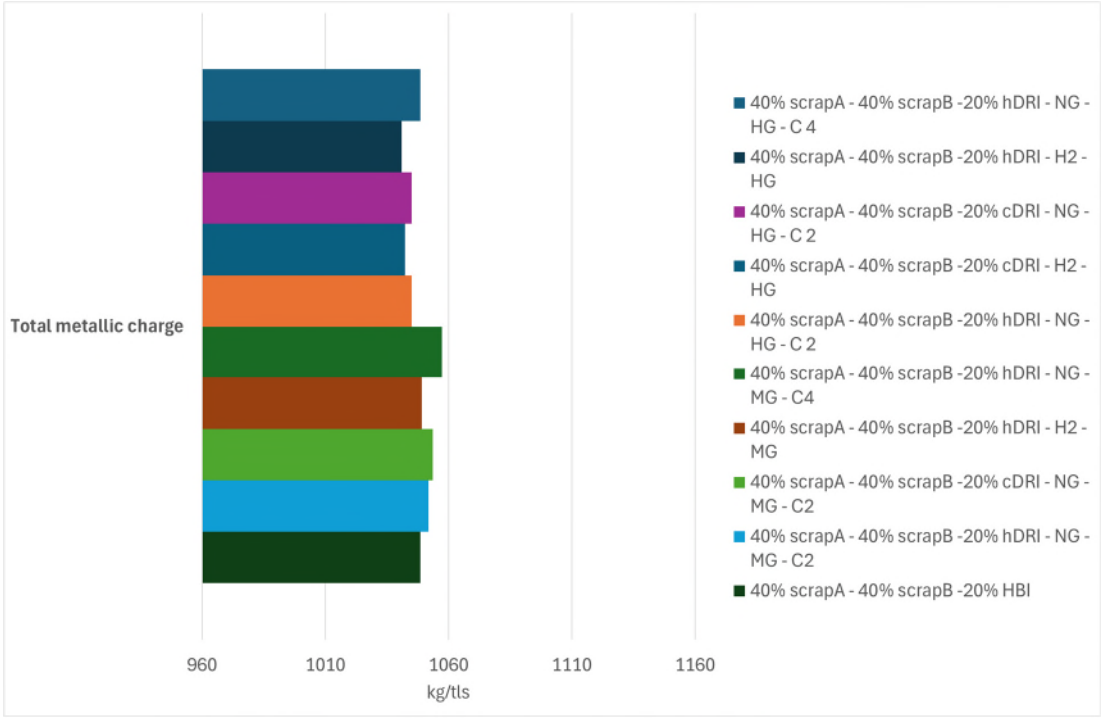

Figure 28 Variation of specific total metallic charge with different type of iron bearing materials (**Scenarios D**)

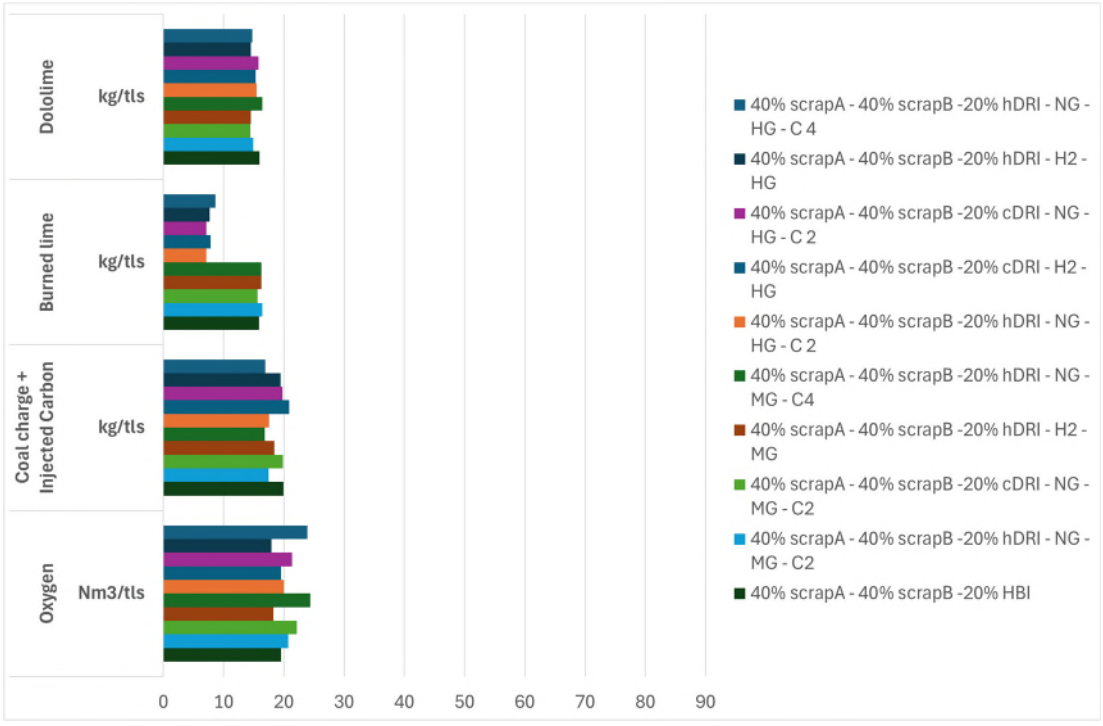

Figure 29 Variation of other specific inputs with different type of iron bearing materials (**Scenarios D**)

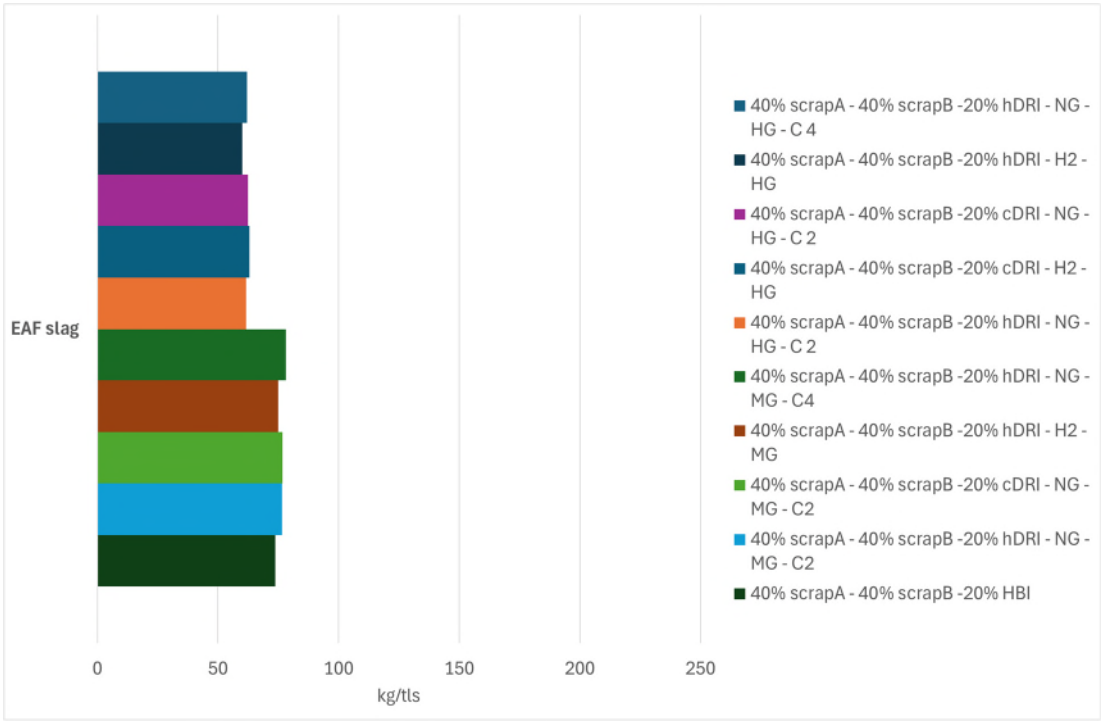

Figure 30 Variation of specific EAF slag amount with different type of iron bearing materials (**Scenarios D**)

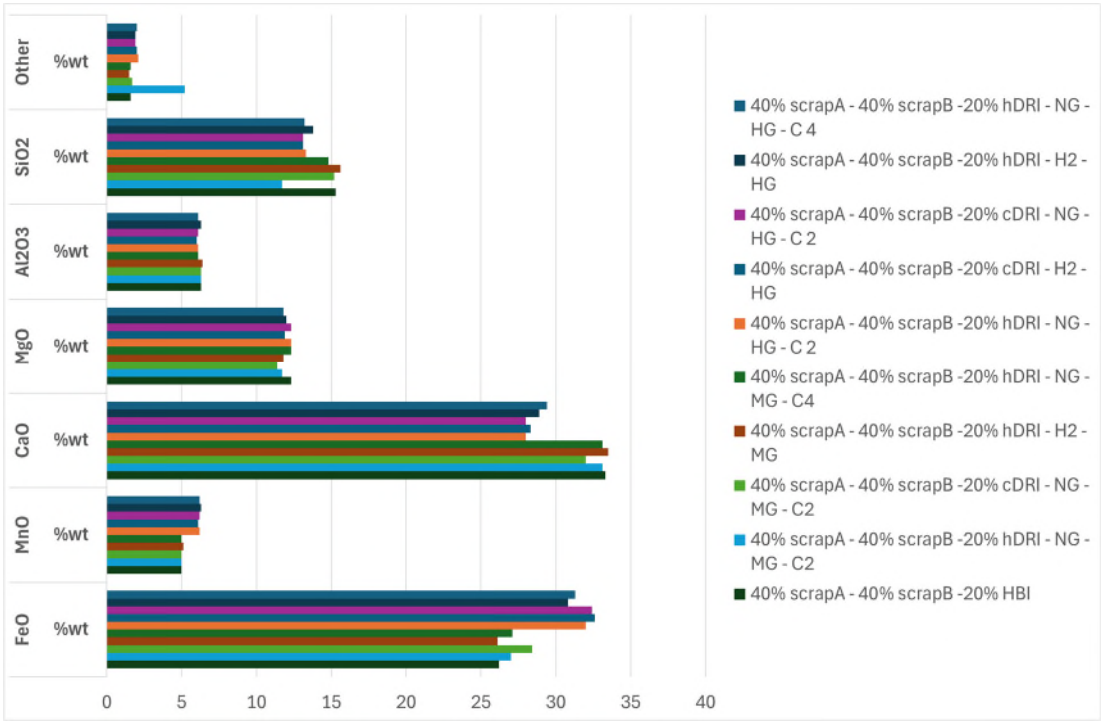

Figure 31 Variation of EAF slag composition with different type of iron bearing materials (**Scenarios D**)

At the end of carried out scenarios, the following conclusion can be reached: severity of the effects depends on the amount and qualities of the used alternative iron bearing material, process and product

types, and set specifications (since they decrease the degrees of freedom). A good compromise must be found in the replacement of scrap with particular qualities of DRI/HBI to avoid undesired effects on slag and steel, and/or major impact on the process.

5.1.2 ESF

The defined scenarios foresee the ESF-based production of hot metal with the features reported in **Table 4** and the use of the same alternative iron bearing materials (single or mixed) considered in EAF **Scenarios C** and **D**. The aim is like the EAF Scenarios, i.e. evaluating slags and process needs with provided specifications.

Table 4 Hot Metal specifications for ESF scenarios

Variable	UoM	Value
Total Fe	wt%	95
Metallic Fe	wt%	95
C content	wt%	3.5
Si content	wt%	0.5
P content	wt%	0.05
S content	wt%	0.01
Temperature	°C	1400

These scenarios will be performed after the finalization of ESF model tests.

5.2 Dynamic EAF simulations

Two sets of scenarios were simulated by CRM with dynamic EAF model.

5.2.1 First set of scenarios : DRI quality

The first case that was simulated was about DRI quality and its impact on slag features. For this set of calculation, the base case was extracted from historical data of an industrial EAF of 220 tons capacity, equipped with 2 oxygen lances and no burner. The specific heat taken into account had a tap weight of ~200 tons, a tap to tap time of slightly less than 1h and only one O_2 lance was used. The DRI contained 2% carbon and 90% iron (metallization degree of 94%), rest was the gangue. The operating pattern of this specific heat is shown in **Figure 32**

This specific heat was chosen, among other reasons, because the heat was part of a series in which the slags were sampled and analysed and the correlation with model prediction was ensured. For this specific heat, the slag composition was the one given in **Table 5**.

Table 5 Slag composition for the first base case for EAF model simulation

%FeO	% SiO_2	%CaO	%MgO	%Al_2O_3	IB2
34	15	37	10	3.5	2.5

Starting with this base case, two modification of the DRI were taken into account for the simulations: (i) a decrease of the carbon content (to 0%) to represent hydrogen reduction and (ii) a lowering of the DRI quality by decreasing the total iron content and the reduction degree.

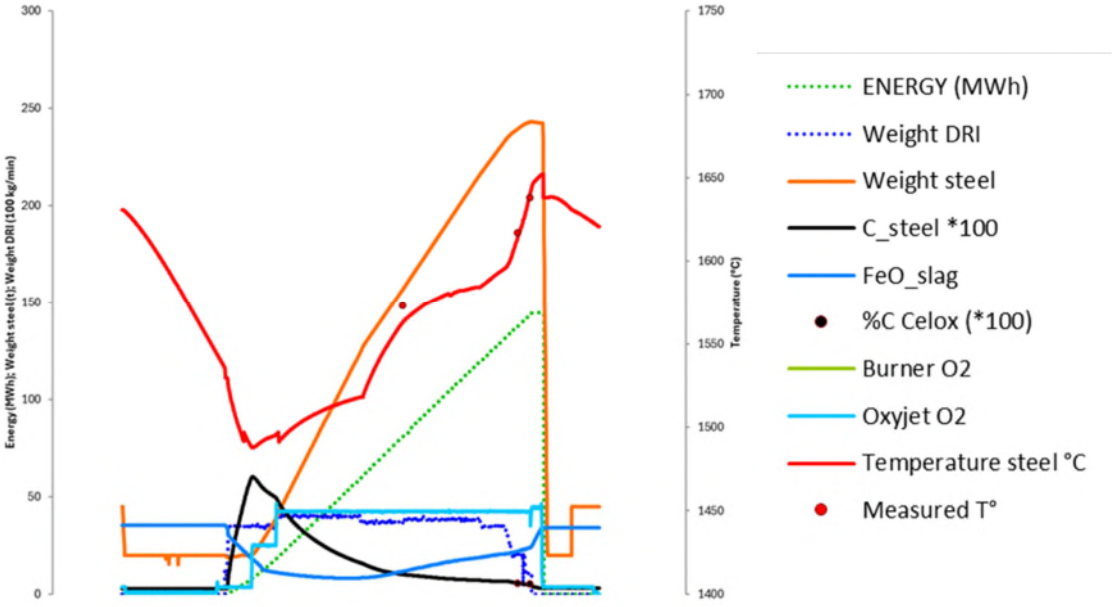

Figure 32 Operating pattern of first base case for EAF dynamic model simulation

0% carbon DRI

The first adaptation of the DRI was to reduce its carbon content from 2 to 0%, keeping the rest in the same relative composition.

Figure 33 shows the impact of the reduction of carbon in the DRI on the EAF process. Due to lower carbon, the initial melting temperature is higher and the final steel temperature is lower for the same injected energy. FeO in slag is also much higher as its reduction from slag is reduced. On the same figure, the last graph depict an adaptation of the process to deal with the lower carbon content of DRI, replacing it by a bulk charging of coke at the beginning of the heat. The adaptation allows to recover a behavior similar to the initial one despite a globally higher carbon usage due to a less efficient action for the reduction of FeO.

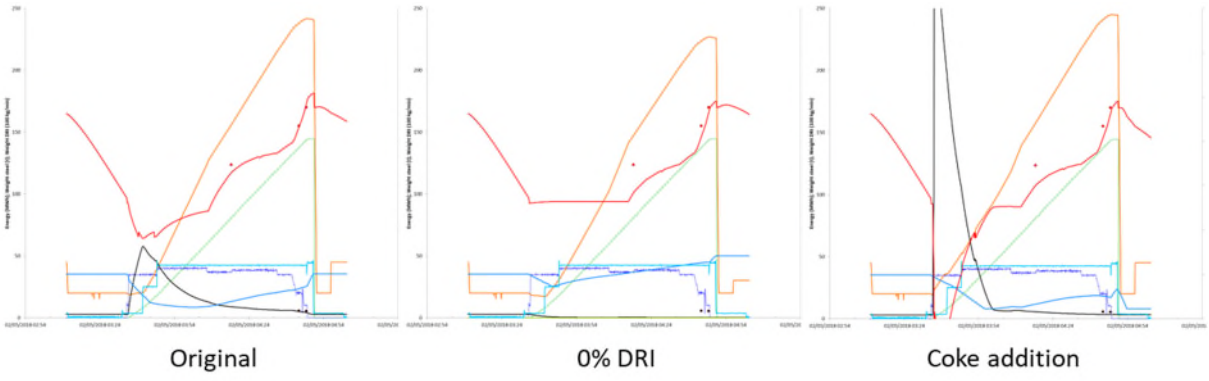

Figure 33 Impact of carbon reduction in DRI and adaptation of operation

On **Figure 34** are depicted the steel and slag produced during the heat for the three simulated cases (left graph) and the slag composition for each of them (right graph). As expected, by lowering the carbon

content in the DRI without modification of the process, the slag ratio is consequently increased. This quantity increase is mainly iron oxide what explains the increased of FeO in the slag composition with proportional decrease of the other elements. By adding coke at the beginning of the heat to replace the missing carbon, the slag ratio could be recovered. Nevertheless, the slag composition, for its part, is not really the same than the initial one because the behavior of the added carbon is not the same than the one in the DRI and is more prone to carburize the bath and less to reduce iron oxides than carbon from DRI.

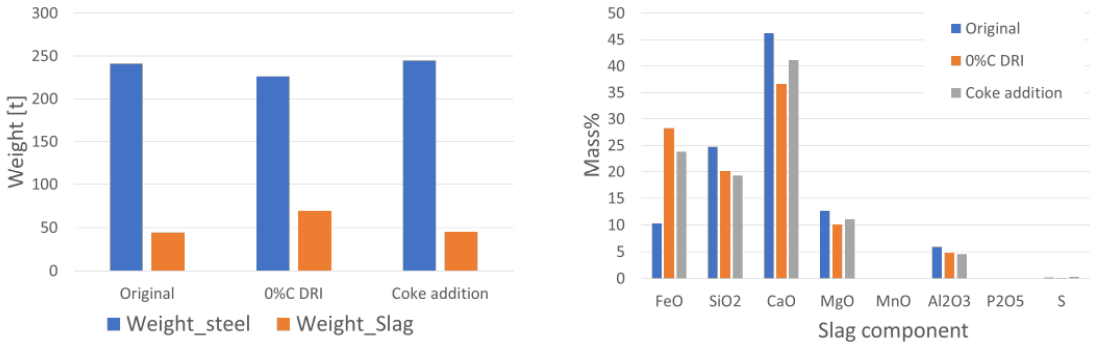

Figure 34 Steel/slag weight and slag composition in function of carbon in DRI

Lower quality DRI

The second set of calculation was performed using a numerically decreased quality of the DRI. Two parameters were taken into account, the total iron content and the metallization degrees, considering the initial DRI as highest quality. The initial iron content of 90% was reduced to 85% and the initial metallization degree of 94% was reduced to 90 and 85%. The trials will be referred as:

- 90Fe94M → 90% total iron, metallization degree of 94% (base case)
- 90Fe90M → 90% total iron, metallization degree of 90%
- 90Fe85M → 90% total iron, metallization degree of 85%
- 85Fe94M → 85% total iron, metallization degree of 90%
- 85Fe94M → 85% total iron, metallization degree of 85%

In **Figure 35** are given the steel and slag produced during the heat for the three simulated cases and in **Figure 36** the slag composition for each of them. Decreasing the total iron content or the metallization degree both tend to increase the slag rate with increase of produced slag and decrease of tapped steel. Similarly, both modifications result in increased iron content in slag. The rest of the slag composition is driven by the gangue composition/content and the lime addition.

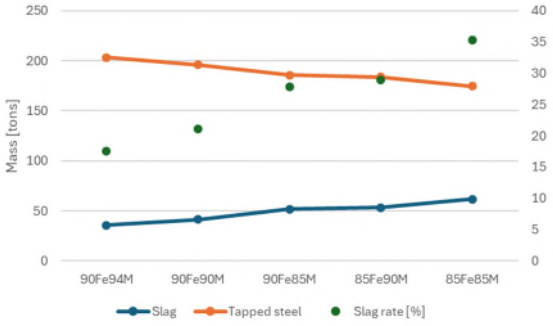

Figure 35 Steel/slag weight in function of DRI quality

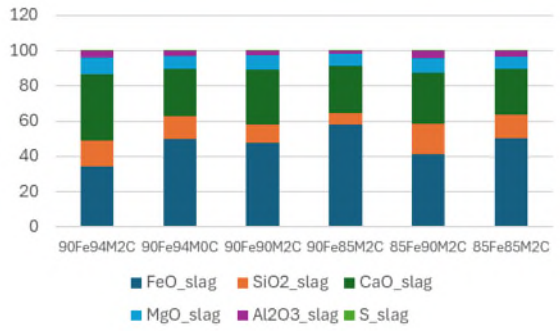

Figure 36 Slag composition in function of DRI quality

Similarly to what was done for low carbon DRI, the process could be adapted to partly recover similar performances than initially. Nevertheless, as depicted on **Table 6**, these adaptations result in significant increase of energy consumption and (injected) carbon addition while still lower iron yield is observed. This is mainly because the EAF is operating under oxidizing conditions. In case of the ESF with reducing conditions inside the furnace also higher carbon and energy consumption will be necessary for lower metallization and lower C in DRI but higher iron yield can be achieved.

Table 6 Process modification in case of lower DRI quality

	C addition	Iron yield	Energy
	Δ [kg/t]	[%]	Δ [kWh/t]
90Fe94M		91	
90Fe90M	5.3	89	13
90Fe85M	12.1	88	25
85Fe90M	3.7	83	56
85Fe85M	10.0	82	68

5.2.2 Specific scenarios definition

The specific cases to be simulated have been defined in accordance with ArcelorMittal to be in line with one of the expected future EAF operation for flat products. These simulations are based on the following:

- 2 DRI composition of various qualities
- One reference scrap quality (E3)
- 2 extreme scrap/DRI ratios (20-80% and 45-55%)
- Very low P in steel (more stringent parameter in this scenario)
- Slag basicity > 2
- MgO in slag ~7%

From the defined base case, simulations had been run keeping constant the %C in steel, the %P in steel and the tapping temperature by adapting (among others) the lime and dolo-lime addition, the oxygen blowing, the foaming coal injection and the electric energy.

The main characteristics of the DRIs made from high grade iron ore considered for the calculations are given on **Table 7**. Both have roughly the same metallization degree but the total iron content is higher

in the first one. The second also contains ~10 times more phosphorus. Finally, the basicity of the first DRI gangue is lower.

Table 7 DRI features

Compounds	High qual. DRI	Mid qual. DRI
C	2.7	2.30
S	0.003	0.003
P	0.009	0.090
C/S ratio	0.35	0.80
C/A ratio	1.35	4.25
Fe tot	91.2	88.7
Met. Degree	94.0	94.0

In complement of DRI, E3 scrap have been used. Their composition was taken in accordance with EU specification for this grade (**Table 8**).

Table 8 E3 scrap grade specifications

	Cu	Sn	Cr, Ni, Mo	Dimensions	Density	Sterile
E3	≤ 0.25	≤ 0.01	∑≤ 0.25	Thickness ≥ 6mm <1.5x0.5x0.5m	≥ 0.6	≤ 1%

A set of simulations was performed with a variable scrap/DRI ratio. For each one, the process parameters (lime and dolo-lime addition, oxygen blowing, coal injection, electric energy…) have been adapted in order to keep the expected outcomes (%C, %P and %S in steel, taping temperature, tap to tap time) constants. The results of the calculations are given on **Figure 37 and Figure 38** here below. Figure 37 depicts the slag composition for each case and **Figure 38** the respective slag weight and basicity.

Unintuitively, the slag amount decreases when the DRI ratio increases. This is due to the lower need of lime addition to remove phosphorus and sulfur (already low in the DRI) and dolomite (as DRI already contains MgO). Oxygen blowing was also more intensive for the cases containing less DRI to correctly burn residuals from scrap (P, Si, Mn…) what explains the higher FeO content. The slag composition is also driven by the slag conditioner addition and lower DRI cases contain more CaO as more was added. Slag from high DRI cases contain more SiO_2 due to the DRI gangue itself.

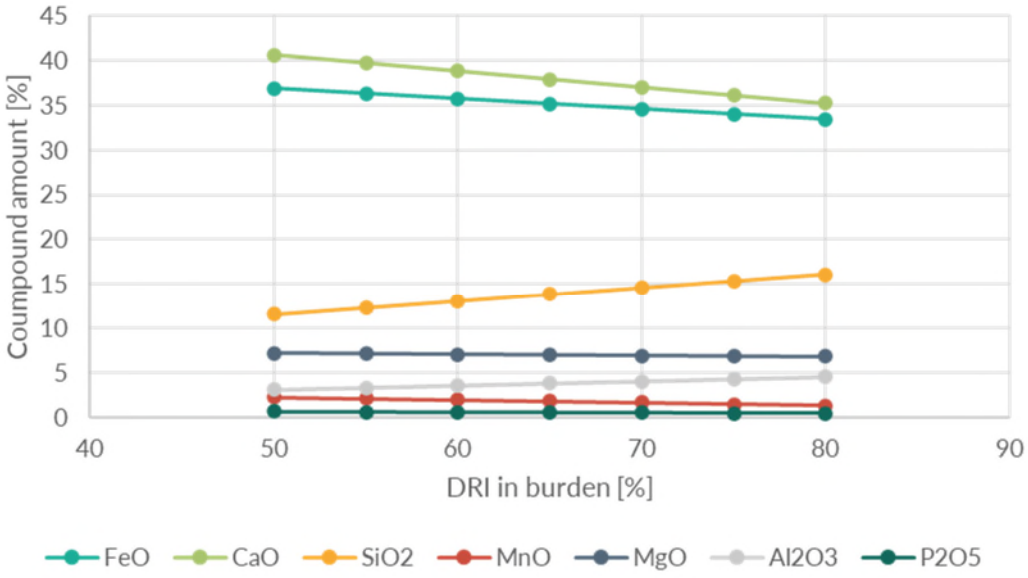

Figure 37 Slag composition in function of DRI ratio for high quality DRI

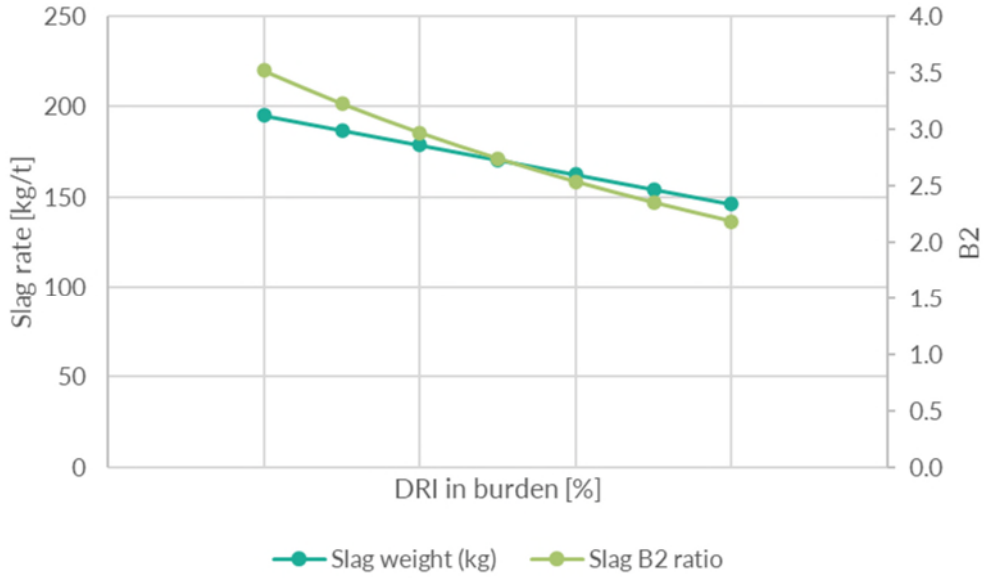

Figure 38 Slag weight and basicity in function of DRI ratio for high quality DRI

Similar calculations were performed using medium quality DRI. The results are given in **Figure 39** and **Figure 40**. The comments are quite similar to the previous case but the slopes are weaker as the slag amount is in any case higher than for high quality DRI. All the effects are therefore diluted. The basicity of the DRI gangue being higher, less lime was necessary (slag basicity is in any case higher than expected) specifically for that.

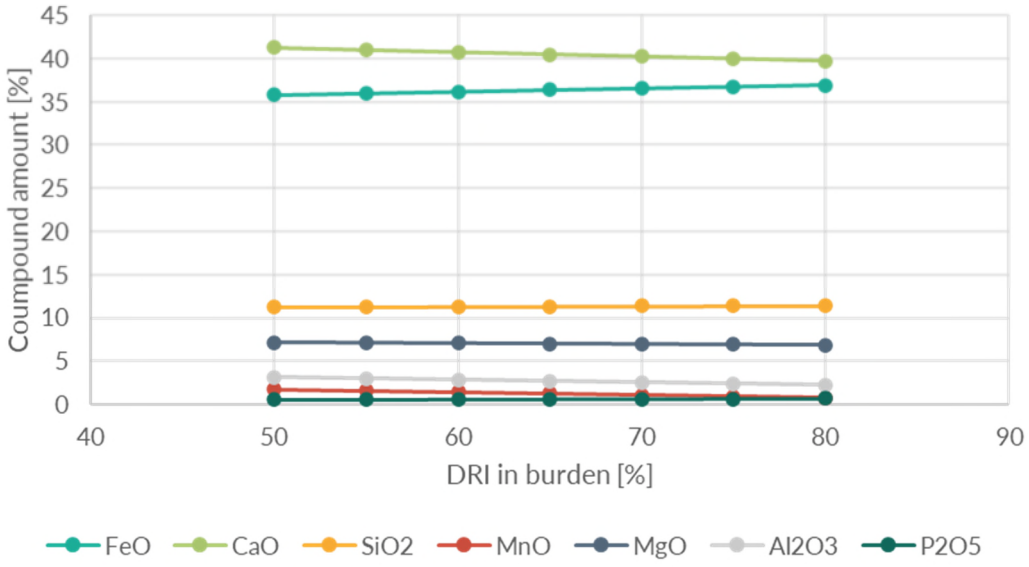

Figure 39 Slag composition in function of DRI ratio for medium quality DRI

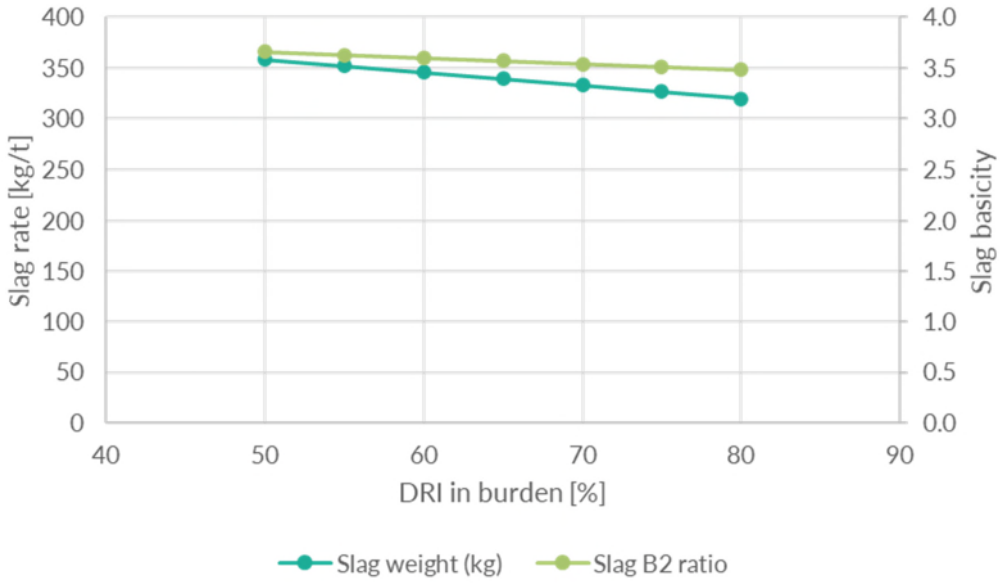

Figure 40 Slag weight and basicity in function of DRI ratio for medium quality DRI

In **Figure 41**, the slag composition obtained for both DRI grades with a DRI rate of 80% are given. These compositions will be used as reference for further lab/pilots trials.

It should be noted that these results are related to a specific study case and cannot be considered as representative of the general impact of DRI ratio in the burden mix. The goal of the simulation was to define the slag composition of one (among others) realistic scenario envisaged by ArcelorMittal as a possibility in the future steel production.

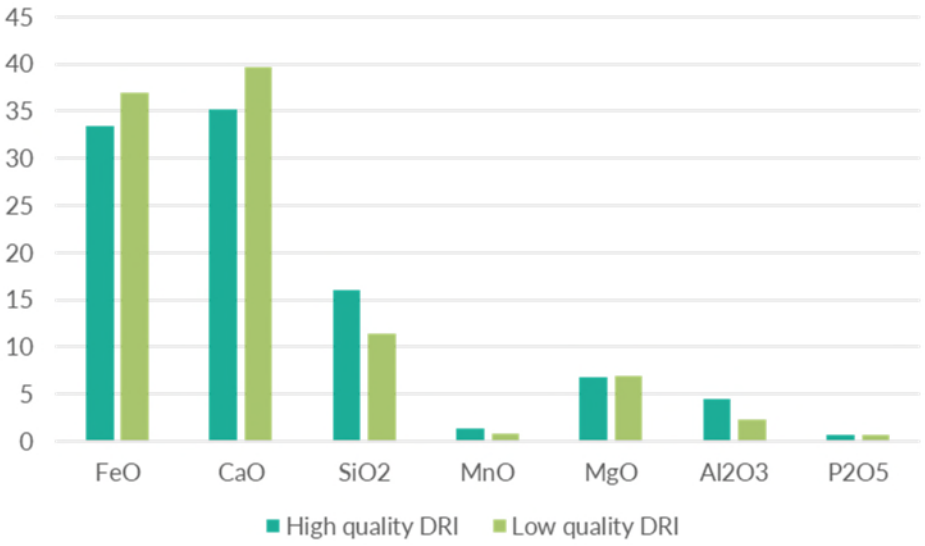

Figure 41 Slag composition for 80% DRI for both qualities of high grade DRI

6 Conclusion

Two EAF models have been presented, adapted and used to conduct several investigations on the effects of the use of different qualities and ratio of DRI and HBIs on EAF slags. In addition, an ESF model was presented that will be used in the project for similar investigations.

The studies considered different production processes, different EAF units, DRI and HBI qualities and produced steel grades. An extensive overview and understanding of the possible EAF slag changes in future operations is provided.

It was found that the severity of the effects depends on the used DRI/HBI ratios, qualities and compositions, process and product types, and set specifications. Generally, lower quality DRI leads to the increase of slag amount, to higher compositions changes and to slag acidification with possible consequences on the removal of undesired elements for steel. Some extreme investigated cases lead to the production of slags not suitable for correct industrial operations. However, process and slag adaptations were proposed to achieve the correct process operations and slag features.

With suitable compromises in the ratios and qualities of alternative iron bearing materials used in EAF process and with ad-hoc designed process changes, both process, product and slag targets can be ensured.

Although the interesting results and provided extensive overview, it is important to highlight that the carried out analysis cannot be considered exhaustive and representative of the general impact of DRI/HBI ratio and qualities in the EAF process, product and slag. They can provide insights on slag obtained in future EAF operations and guidelines for obtaining a smooth transition and operation with new feedstocks and can pave the way for further studies.

InSGeP

Investigations of Slag from Next Generation Steel Making Processes

START DATE | 01-07-2023
PROJECT DURATION | 48 months
TOPIC | RFCS-02-2022-RPJ
BUDGET | 4.5 M€
COORDINATOR | FEhS
CONTACT | info@insgep.eu

The information and views set out in this document do not necessarily reflect the official opinion of the European Commission. The European Commission does not guarantee the accuracy of the data included in this document. Neither the European Commission nor any person acting on the European Commission's behalf may be held responsible for the use which may be made of the information contained therein.